COMPUTATION OF ELECTRICAL EFFICIENCY OF BLDC MOTOR OF CHITRA LVAD

A Thesis

Submitted By

Akash Dhetarwal

For the award of degree of

MASTER OF TECHNOLOGY, CLINICAL ENGINEERING

Jointly offered by

Indian Institute of Technology, Madras

Christian Medical College, Vellore

Sree Chitra Tirunal Institute for Medical Sciences and Technology, Trivandrum

June 2022

CERTIFICATE

This is to certify that the thesis titled '**COMPUTATION OF ELECTRICAL EFFICIENCY OF BLDC MOTOR OF CHITRA LVAD'** being submitted by **Akash Dhetarwal** to SCTIMST Trivandrum, for the award of degree of **Master of Technology in Clinical Engineering** jointly offered by IIT Madras, CMC Vellore and SCTIMST Trivandrum, is a bona fide record of research work done by him under my supervision. The contents of this thesis in full or in parts have not been submitted to any other Institute or University for the award of any degree or diploma.

The research had been carried out at Biomedical Technology Wing of Sree Chitra Tirunal Institute for Medical Sciences and Technology (SCTIMST), Trivandrum.

Mr. Sarath S. Nair

Guide

SCIENTIST 'E'

Division of Extra-corporeal Devices,

SCTIMST, Trivandrum

Abstract

Congestive heart failure is a major cause of morbidity and mortality as well as a major health care cost in the developed world. There are highly effective heart failure therapies which are introduced such as Cardiac Resynchronization Therapy (CRT). They reduce the mortality and can improve the function of the heart that leads to improve the quality of the life. There are large number of patients who do not respond to these therapies. For such type of patients, transplantation of the heart is an option but that is also limited because of the donor availability as well as co-morbidities which may also limit survival post-transplant. To avoid these problems in the transplantation therapy, clinicians are forced to adopt or think about some alternative measures. Employment of Mechanically Circulatory Devices is one of such promising measures. Mechanical Circulatory Devices particularly, Left Ventricular Assist Devices (LVADs) are the topic of discussion for they can be the best alternative to improve the failing left heart. As promising as they sound, there are many numerous fields that need to be taken into consideration in developing a better Mechanical Circulatory System (MCS).

The purpose of this study is to evaluate the electrical efficiency of the Chitra Left Ventricular Assist Device (LVAD) that is under developmental stages in the SCTIMST institute. The study is focused on the major performance parameters of the pump and the motor used in the pump such as pump inlet and outlet Pressure difference (ΔP), Flow, Torque, input power, output power and electrical efficiency that are studied by a set of experiment organized to be performed. The Torque value of the LVAD was computed using an experimental set-up as well as in ANSYS CFD simulations and the error in the results was recorded. The pump was studied at multiple range of speed varying at different rpm and the electrical efficiency was calculated.

Keywords

Congestive Heart Failure, Mechanical Circulatory Devices, Left Ventricular Assist Device, Impeller, Continuous Flow, Centrifugal Pump, magnetic levitation, Hydrodynamic Thrust, Pressure Head, Flow Rate, Torque, Efficiency, Electrical Efficiency, Simulations.

Table of Contents

List of Figures

List of Tables

Abbreviations

HF - Heart Failure

LVAD- Left Ventricle Assist Device

RVAD- Right Ventricle Assist Device

HFrEF - HF with reduced ejection fraction

HFpEF - HF with preserved ejection fraction

HFmrEF - HF mid-range ejection fraction

LVEF- left ventricle ejection fraction

RAAS - renin-angiotensin-aldosterone system

CRT- cardiac resynchronization therapy

NYHA - New York Heart Association

GDMT - Guideline Directed Medical Therapies

NIH- National Institute of Health

TAH- Total Artificial Heart

VADs- Ventricle Assist Devices

BTT- Bridge-to-transplant

REMATCH- Randomized Evaluation of Mechanical Assistance for the Treatment of Congestive Heart Failure

PM – Power Module

OMM- Optimal Medical Therapy

CF- Continuous Flow

DT- Destination Therapy

INTERMACS- Interagency Registry for Mechanically Assisted Circulatory Support

RV- Right Ventricle

MAP- Mean Arterial Pressure

CFD- Computational Fluid Dynamics

RPM- Rotation Per Minute

Acknowledgements

I would like to acknowledge and give my warmest thanks to my project guide Mr. SARATH S NAIR (Scientist/Engineer -E), Division of Extracorporeal Devices, Biomedical Technology Wing, SCTIMST for the continuous support, patience, motivation, enthusiasm, and immense knowledge. His guidance helped me in all the time of research and writing of this thesis. His high standards have made me better at what I have done and what I will do.

My sincere thanks also go to NAGESH D S (SIC & Scientist-G(Sr-Gr)), VINODKUMAR V (Engineer -F), SARATH G (Scientist-D), AMRUTHA C (Scientist-C), Dr. CHHAVI GUPTA (Engineer-C), SREEDEVI V (Technical Assistant) for sharing their immense knowledge in the field of medical devices and guiding me through the technical difficulties I faced throughout the course of this project.

I express my sincere gratitude to Dr. RAMESH P (Scientist-G & HOD, DMDE, BMT Wing, SCTIMST), Dr. ROY JOSEPH (Course Coordinator SCTIMST), Dr. MANOJ KUMAR (Course Coordinator IIT Madras), Dr. SHIVA KUMAR BALASUBRAMANIAN (Course Coordinator, CMC Vellore) for coordinating this course.

I also express my sincere gratitude to Dr. HARIKRISHNA VERMA (HEAD, BMT WING SCTIMST) for allowing me to do project in BMT Wing SCTIMST for my MTech Studies.

I would also like to thank all the Project staff of Division of Extracorporeal Devices especially Mr. Midhun, Mr. Sudheesh, Mr. Adarsh, Mr. Amith and Mr. Akshay for sharing their skills that helped me to complete my project.

Last but not least, I would like to thank my family for supporting me spiritually throughout my life.

Chapter I

Introduction

Heart Failure (HF) or more specifically End stage Heart Failure is a major cause of mortality and considered as a major cardiovascular disease that leads to global healthcare problem. There are many disorders that leads to myocardial dysfunction and finally may end up in heart failure. Generally, HF can be defined as an improper cardiac output to fulfill the metabolic demands. As it is stated by the Global public health Burden of heart Failure [4], an estimated 64.3 million people living around the world are having various heart problems. More than 26 million people are suffering from chronic heart failure which included around 4.6 million Indian nationals as well. The type of treatment provided for these patients depends on the degree of heart failure and its availability. When compared to the optimal Guideline Directed Medical Therapies (GDMT) the heart transplantation would be the most preferred one [1]. However, the limited availability of donor heart and the increasing heart failure limits the therapy of heart transplantation to a small patient population which lead to the development of artificial hearts. As ventricles of the heart perform the main task of pumping blood throughout the body, the chance of its failure is very high. Hence, instead of implanting a full-fledged heart, it would be required to support the damaged ventricular support in most of the patient cases. Ventricular Assist Device (VAD) is such a form of artificial heart which pumps blood from ventricles of the heart to rest of the body thereby reducing its effort.

VADs are classified as Left Ventricle Assist Device (LVAD) and Right Ventricle Assist Device (RVAD) depending on the location of the ventricle which is assisted. LVAD is a device attached with left ventricle to supports the systemic circulation whereas RVAD is a device attached with the right ventricle to support pulmonary circulation of the body. Both LVAD and RVAD are miniature pumps incorporating similar technologies but operated with the different hydraulic outputs to match with the physiological requirements. In this thesis, an LVAD is considered for further study as well as analysis and the same approach may be adopted for RVAD and other similar heart assist devices.

The LVAD is connected parallel to the systemic circulation loop, where the inlet is connected to the apex of the left ventricle and outlet let is fixed to the ascending aorta through the outflow graft. With the help of LVAD oxygenated blood is supplied to the rest part of the body through arteries. The LVADs may be configured to use as Destination Therapy (DT), Bridge-To-Transplant (BTT),

Bridge-To-Recovery and Bridge-To-Candidacy which depends on the physical ability of the patient. In Bridge to Candidacy therapy, the LVAD is put to a patient waiting for decision on the modality of treatment to be undergone. In the Bridge to Recovery, the device is implanted to patients for a few days to week such that, the patient' heart can rest and allowed to recover with the help of medications. In Bridge to Transplant, the LVAD supports the patient until a donor heart is obtained. When, no treatment failures are available, the LVAD supports the patient as long as it can and this configuration is known as Destination therapy.

Over the years, many research has undergone in the development of the LVAD. The primary objective of the development was to obtain a satisfactory hemodynamic performance with high reliability and survival rate. To obtain these objectives, the LVAD design has gone through numerous generations such as generation I, II, III & IV. According to the type of flow, LVADs are broadly classified into pulsatile flow and continuous flow devices. First generation LVADs such as HeartMate I come under pulsatile flow devices. Second and third generation devices such as HeartMate II and HeartMate III are coming under Continuous flow devices. The second-generation pumps have pivot bearing whereas third generation pump s have magnetic bearings. Many sensors are incorporated in further generations to get the generation V such as Heart Assist where the pump flow can also be measured. More details of these pumps are discussed in the next chapter 'Literature Survey'.

As being a mechanical circulatory support device the LVAD have its own set of complications such as durability and hemolysis and thrombus formation. However, considering the significant clinical impact in HF treatment, further improvement is required to enhance the long-term durability with reduced complications for ultimate acceptance of LVAD. The pump performance parameters have a great impact on durability and complications related to LVAD. The pump performance can be split into two vis a vis hydrodynamic performance and hemodynamic performance. The hydrodynamic performance deals with pressure head, flow rate and the efficiency of the device whereas the hemodynamic performance deals with the hemolysis and thrombus formed within the device. The occurrence of hemolysis and thrombus within a pump are largely attributed to the shear distribution, velocity regime, choice of materials, its surface finish and total surface area of the material. It has been studied that, the occurrence of hemolysis and thrombus can be controlled to a large extent by properly designing the pump thereby limiting the shear and velocity in a particular range. In addition to this performance, the pumps should have good thermal performance parameters as it is implanted in the patient's body. A pump with high heat generation cannot be implanted inside the body as it may produce burns and safety issues. All the current LVADs has an electrical motor to drive the pump which converts the electrical energy

to the mechanical energy. The electrical energy is obtained from implanted batteries or from external kept batteries. The conversion efficiency plays a major role in the design of LVAD as a high efficiency means less loss, reduced battery volume and enhanced battery life. Thus efficiency of the pump is one of the major parameters which has a great impact on pump performance. A pump with high efficiency produces less heat loss and thus have more safety. LVAD has a centrifugal pump which is having two parts mechanical and electrical. Impeller and the casing are come under mechanical part and the motor is the electrical part of the pump. Most of the LVADs are having Brushless Direct Current (BLDC) motor because of their certain advantages such as high efficiency and good speed and torque characteristics. BLDC motor are also called as electronically commutated motor as it employs electronic commutation instead of brushes and slip rings.

One of the major factors that affects the efficiency of the pump is the motor used in it. These motors are integrated within the LVAD and cannot work independently. It is thus imperative to study the efficiency of the motor to have a pump with good performance parameters that lead to have a better durability and the function of the device. Efficiency of the motor used in LVAD is a combination of the hydraulic as well as electrical efficiency of the motor.

The division of Extracorporeal Devices in BMT wing at Sree Chitra Tirunal Institute of Medical Science and Technology is developing a Continuous Flow (CF) LVAD named as Chitra LVAD. This study is based on the fact that electrical efficiency has some impact on the performance parameter of the pump. It has quantified and computed the electrical efficiency of the BLDC motor used in Chitra LVAD. The results that were obtained from the experiments has provided the most suitable speed for efficient operation of the pump. To achieve this torque of the motor was computed with the help of experiments that were performed in the laboratory. The results are validated with the simulation results that were computed in ANSYS CFD simulation software. The detail of the study has explained in the further upcoming chapters.

1.1 Significance and Scope

In this project, the electrical performance of the Chitra LVAD motor is computed through computational as well as experimental methods and documented. The method developed as part of the project enables to study and compare different motor technologies which can be incorporated in the Chitra LVAD. The most appropriate motor technology may be selected considering the torque and efficiency. A CFD model of the pump as well as a test setup is developed to do the analysis. Experimental and the simulation testing were performed and the output at different speeds were recorded to evaluate the performance parameters of the pump.

1.2 Thesis Outline

The thesis is divided into six chapters. Chapter II discuss the history, technological developments in the mechanical circulatory systems, basics of heart failure which give the insight of general information of the heart. Further, the Chapter II includes the principle behind the technology, design features and development of LVAD along with its different generations. Chapter II also discusses about the different materials used in various components of LVAD. Chapter II not only gave the idea of pump mechanism but also explained the other components that go into implantation and how they are used. Further, in Chapter III, the primary objective is sub-divided into secondary objectives. The details of process of torque computation with the help of computational fluid dynamics are explained in chapter IV. The details of methodology adopted for experimental analysis and the procedure for the experiment is explained in chapter V. The results obtained, conclusion drawn and future work are discussed in chapter VI. In the last the references taken are mentioned.

Overall, the thesis gives the detailed idea about the computation of torque, head difference, H (Pressure)-Q (Flow) curve and electrical efficiency of BLDC motor used in Chitra LVAD from simulation and experimental analysis.

The content described in next chapters are pictorially represented in the flow chart in figure 1.1.

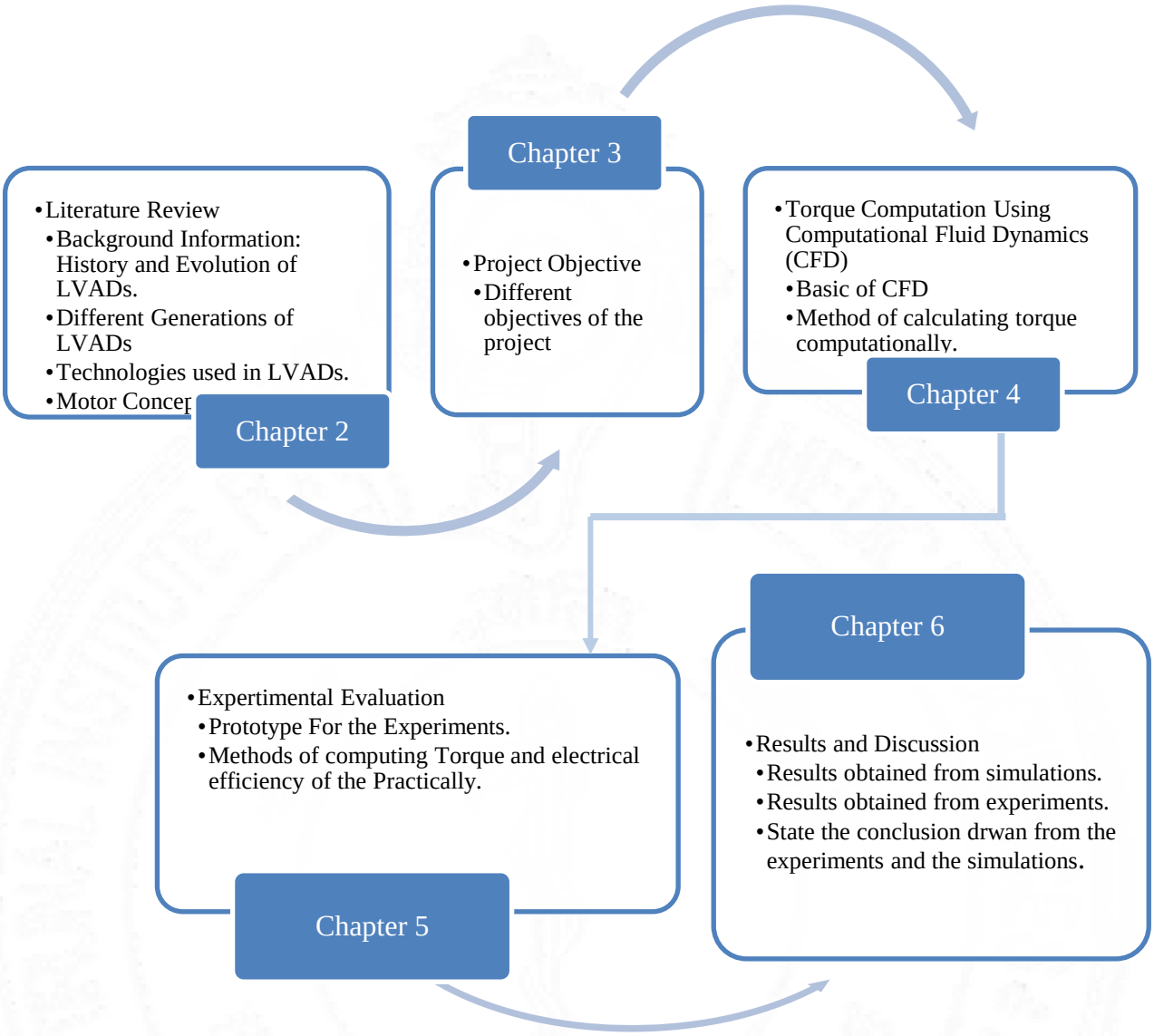

Figure 1.1 Block diagram of flow of study

Chapter II

Literature Review

This chapter presents the existing literature on Left Ventricle Assist Device (LVAD). It has been divided into two parts. The first part describes about history and evolution of different generations of LVAD, Components, Materials, technology and complications related to LVAD. Second part focuses on the electrical parts of the LVAD such as motor. It provides the basic overview of motor dynamics and the motor used in Chitra LVAD.

Howard J. Eisen.et al. under the study, 'Left Ventricular Assist Devices (LVADS): History, Clinical Application and Complications' [1] stated that the major cause of morbidity and mortality in the world is the congestive heart failure. There are highly effective medical therapies such as Cardiac Resynchronization Therapies (CRT) are there which reduces the mortality and improve the cardiac function. There are large number of patients existed who do not respond to these medications and therapies. According to the ejection fraction, HF has been classified into three subtypes, namely HF with reduced ejection fraction (HFrEF), HF with preserved ejection fraction (HFpEF) and HF mid-range ejection fraction (HFmrEF) which is shown below in the figure 2.1.

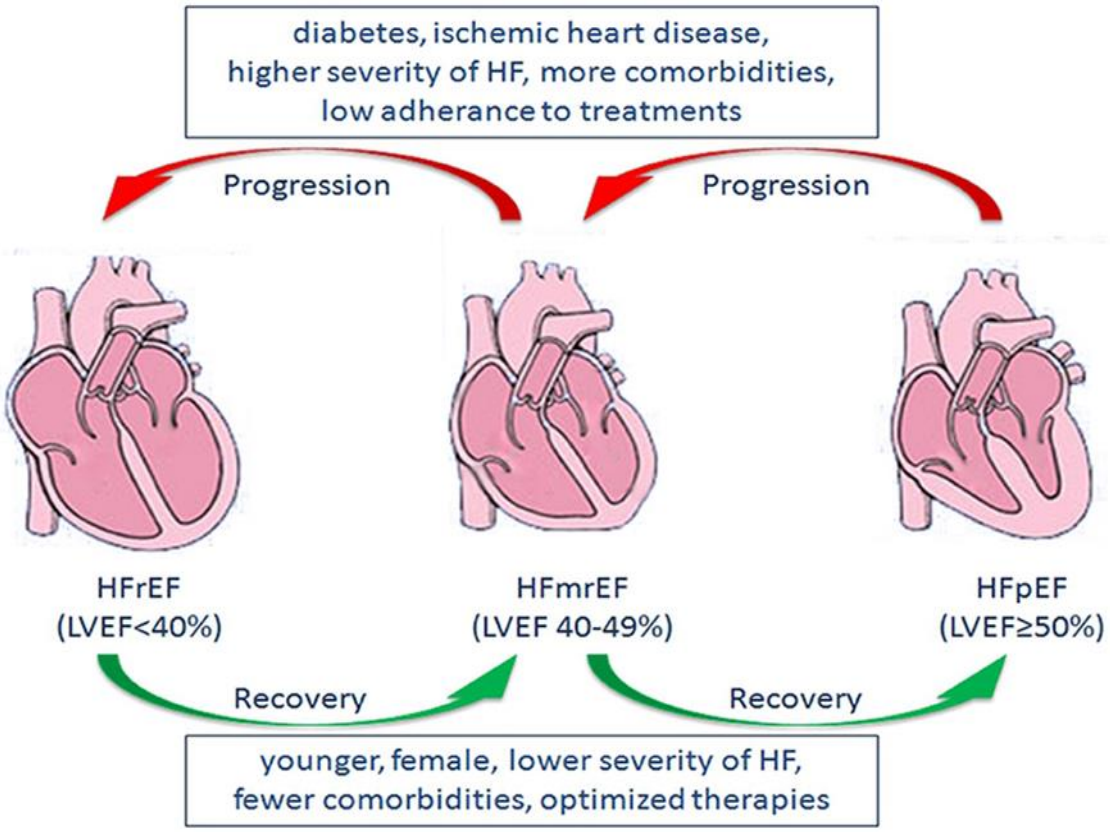

Figure 2.1 Classification of Heart Failure[13]

Heart failure with reduced ejection fraction (HFrEF) can be defined as a left ventricular ejection fraction (LVEF) less than 40%, heart failure with preserved ejection fraction is defined as a LVEF greater than or equal to 50% and heart failure mid-range ejection fraction can be defined as LVEF in between 40 % to 49%. LVAD therapy is generally used for patients with HFrEF and who have failed Guideline Directed Therapies that included renin-angiotensin-aldosterone system (RAAS) antagonists, sympathetic nervous system antagonists and cardiac resynchronization therapy (CRT) with bad symptoms and cardiac dysfunction. There are Patients with New York Heart Association (NYHA) class IV symptoms (dyspnea at rest). NYHA heart failure classification is shown below in the figure 2.2.

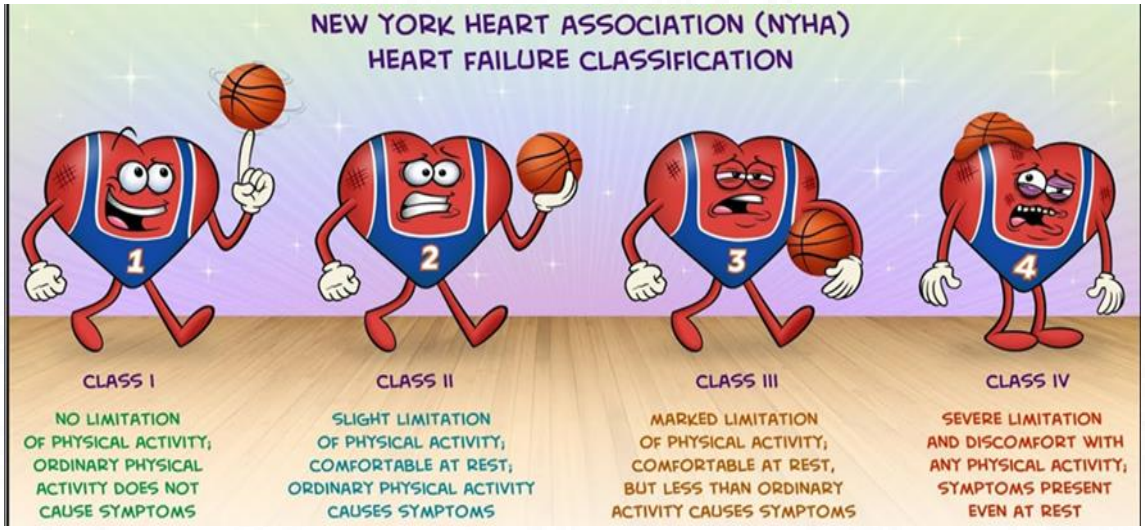

Figure 2.2 New York Heart Association Heart Failure Classification[12]

Despite optimal Guideline Directed Medical Therapies (GDMT) Class IV have a poor prognosis at one year as well as a poor quality of life. They required more advanced therapies such as heart transplantation or LVADs. These types of patients were categorized as advanced heart failure patients. For such type of patient, cardiac transplantation is an option but that is also limited by donor availability as well as co-morbidities which limits the survival after transplantation. For those patients LVAD was used as an alternative that has been used to improve survival rate and also used as a device that can improve the quality of life. It is considered that LVAD implantation has significant complications and device-related problems that are occurred after implantation. That can also refer to as post implantation complications. These complications are discussed later in this chapter.

2.1 History

Howard J. Eisen.et al. under the study, 'Left Ventricular Assist Devices (LVADS): History, Clinical Application and Complications' [1] has described that the earliest effort for the cardiovascular system is to use the external technology to provide cardiopulmonary bypass during cardiac surgery. John Gibbons performed the surgery on a patient who was undergoing atrial septal

defect repair and that led to the interest of National Institute of Health (NIH) for providing support to the patients who was in cardiovascular shock.

Initially the first effort was started to completely replace the heart. In 1950s, at Cleveland Clinic William J. Kolff developed a Total Artificial Heart (TAH). Later, Michal DeBakey has got a grant from NIH to develop a LVAD. The first intention behind making these devices was to provide or to act like a bridge in patients who were having cardiogenic shock until the heart donor was available. The earliest Ventricle Assist Devices (VADs) were Para-corporeal with external VADs which was used for providing blood flow to the patients. The first of these types of devices were implanted in the late 1960s named as pneumatic heart assist device, which was developed by Dr. William Pierce at Penn State University as shown in the figure 2.3. Later, this device was approved by Food and Drug Administration (FDA) which was named as Thoratec Pneumatic VAD for to act as a Bridge-to-transplant (BTT). The device had been used over 4000 patients for ventricular support. Modification in the technology had done and to make it into a pulsatile device named as HeartMate I which was first used as BTT for nearly 25 years.

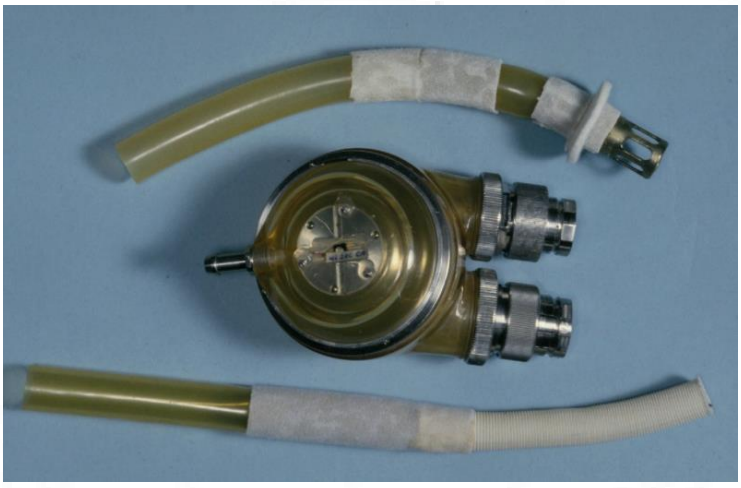

Figure 2.3 The prototype of the first left ventricular assist device. [1]

Jooli Han.et al. under the study ‘Cardiac Assist Devices: Early Concepts, Current Technologies, and Future Innovations’ [3] has described that the first artificial ventricles that were implanted during clinical use was reported by Liotta in the year 1963 which consisted of a pneumatically-compressed tubular conduit with valves that connects the left atrium to the descending aorta.

Joseph A.R. Englert.et.al. under the study, ‘Mechanical Circulatory support for the Failing Heart: Continuous-Flow Left Ventricular Assist Devices’ [2] have shown the development of LVAD technology during past years as given in the figure 2.4.

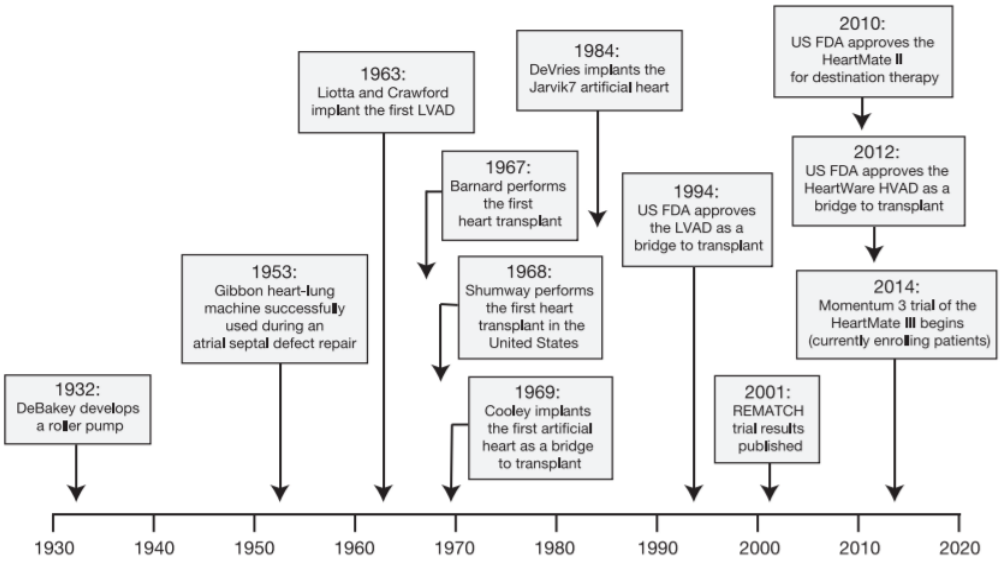

Figure 2.4 LVAD technology evolution. [2]

Howard J. Eisen.et al. under the study [1] has described that the first approach that investigated was Destination Therapy for using LVADs. HeartMate I used as a MCS in the Randomized Evaluation of Mechanical Assistance for the Treatment of Congestive Heart Failure (REMATCH) trial for the patients who were having advanced heart failure. In the trial 129 patients who had advanced heart failure were randomized out of those 68 patients was assigned to provide LVAD and 61 was assigned to provide Optimal Medical Therapy (OMM). In the result it evaluated that the patients who had been provided LVAD had less risk as compared to OMM. Quality of life was also good in patients who had been received LVAD as compare to OMM. Survival rate of 52% were obtained for the patients who were in the LVAD group. LVAD group patients were also had adverse events such as infection, bleeding and device malfunction. Survival of patients who had provided LVAD was far inferior than the patients who was reported for heart transplant.

The outcomes were not that much adequate that could adopt widely. For DT to flourish and benefit a large patient population advanced LVAD was developed. Details of these devices are discussed below.

2.2 Left Ventricle Assist Devices

Joseph A.R. Englert.et.al. under the study, 'Mechanical Circulatory support for the Failing Heart: Continuous-Flow Left Ventricular Assist Devices' [2] has described that initially the devices that were developed had been made to provide the flow in such a way that the devices were replicate the flow of the heart. But the problem was that they were large and noisy, because of that they required large percutaneous leads that were not durable.

Because of large size, more weight and more length of the percutaneous cable requirement. The modification had been done in the past few years. The old pulsatile technology was replaced by Continuous Flow (CF) technology. The benefit observed from the modification is that the devices

with continuous flow was having less weight (almost one quarter), size (one seventh approximately) and less length of percutaneous cable that makes them more durable as compared to the old devices. Joseph A.R. Englert.et.al. during the study' [2] has also described that the mostly second and the third-generation devices were implanted after their development so they completely overtake the old pulsatile devices.

2.3 Basics of CF-LVADs

Second and third-generation devices are having similar function. The main basic components of a CF LVADs are: an inflow cannula, a pump, an outflow cannula, a percutaneous driveline, and an electrical controller as shown in the figure 2.5.

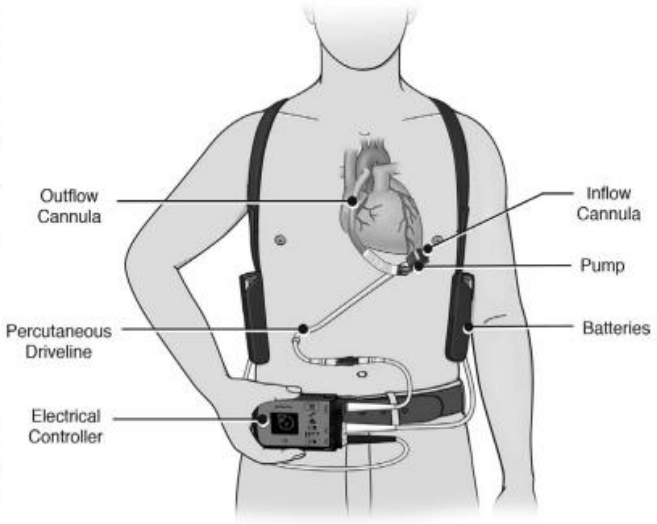

Figure 2.5 left ventricular assist device components. [2]

The inflow cannula is usually inserted into the apex of left ventricle of the heart and the outflow cannula is connected to the ascending aorta. Blood comes to the left side of the heart from lungs and then exits from the apex of left ventricle. Then it goes from the inflow valve into the prosthetic pumping chamber. Blood is then pumped actively into the ascending aorta through the outflow valve. The pumping chamber is located or placed within the peritoneal cavity or abdominal wall. There is also a percutaneous driveline which carries the electric cable and air vent to the battery packs and electronic controls that are worn on a shoulder holster and belt. There are many considerations that can affect the evaluation of a patient for advanced mechanical therapy. Common indications and contraindications for LVADs are described below.

There are two ways in which LVAD can be used:

1. Bridge-To-Transplant (BTT): This is used for the critically ill patients who needs heart transplantation. LVAD can be used as a device to alive a patient until the donor's heart or heart transplant becomes available.

2. Destination Therapy (DT): This is used for the patients who require lifelong MCS as an alternative to heart transplantation.

- **Decision Making Process for LVAD transplantation/implantation:**

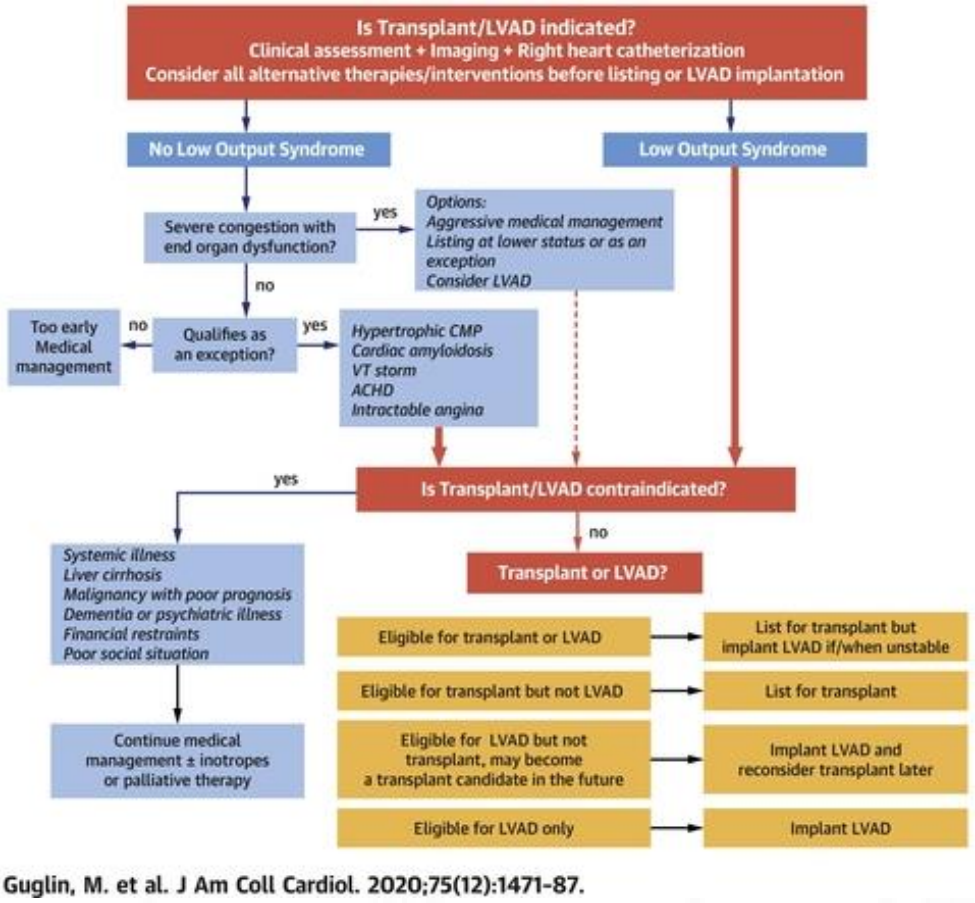

Figure 2.6 Decision making process for LVAD implantation. [5]

- **Indications:** Generally, LVADs are reserved for the patients who have very poor cardiac function and can be able to live only few months. Some of the common indications for getting LVAD are listed below:
  - Patients who having optical medical management failed at least 75% of the time.
  - Patients who are having Intra-Aortic Balloon Pump (IABP) dependency for 7 days.
  - Patients who are having inotropic dependency for 14 days.
  - LVEF<40%
  - Patients having NYHA class IV symptoms (Dyspnea at rest).
- **Contra-Indications:** Generally, based on type of patient's contraindications are classified broadly into two types. Absolute and Relative which are shown below in the table 2.1.

Table 2.1 Contraindications for Mechanically Support Devices

S. No.	Absolute Contraindications	Relative Contraindications
1	Patients who have neurological and Irreversible renal function or renal disease.	Limited life expectancy (age>80 for DT).
2	Medical Non-Adherence.	Poor nutritional status.
3	Severe Psychological limitations.	Limitations to rehabilitation and psychological barriers.

Patient selection and the implant timing are the key determinants of success for LVAD therapy. The severity of cardiac dysfunction and heart failure, timeliness and the necessity of LVAD intervention has been defined using Interagency Registry for Mechanically Assisted Circulatory Support (INTERMACS) profiles [15]. Risk associated during implantation of LVAD can be identified using these profiles. These profiles are important because these indicates that patients belong to profile 1 (severe cardiogenic shock) have the lowest survival and patients belong to profile 3 (stable on inotropes) have the best survival. This type of information can suggest that patient with the profile 1 needs to be optimized their condition before LVAD implantation therapy. The INTERMACS profiles are illustrated below in the table 2.2.

Table 2.2 INTERMACS Profiles [15]

Profile	Description
1	**Critical cardiogenic shock:** Patient is "Crashing and Burning" which means that the patients have life threatening hypotension and having inotropic pressor support which is rapidly escalating.
2	**Progressive Decline:** Patient is dependent on inotropic support but continue to show signs of clinical deterioration.
3	**Stable but inotrope dependent:** Patient is clinically stable on intravenous inotrope doses but cannot be weaned off from the doses.
4	**Resting symptoms:** Patient having oral therapy at home but frequently having some symptoms of congestion when at rest.

5	**Exertion Intolerant:** Patient is comfortable at rest but cannot do physical activity that require more effort so basically can be considered as housebound.
6	**Exertion limited:** Patient is comfortable at rest but quickly become symptomatic with any extra other activity.
7	**Advanced NYHA Class III:** Patient is clinically stable but have some acceptance level of comfortability.

2.4 Basic Components of LVAD

The system components of the MCS are classified into two parts:

1. Internally Implanted Pump: Internally implanted pump which is having following things:
    a. Inflow Cannula
    b. Pump Mechanism
    c. Outflow Graft
    d. Driveline coming out from the abdomen
2. External Components: External components includes following things:
    a. System Controller
    b. Power Sources (Power module, Battery)
    c. Driveline, Percutaneous lead, Power cord
    d. Accessories

Figure 2.7 below is showing the all components in place assisting the left ventricle using the continuous flow centrifugal pump.

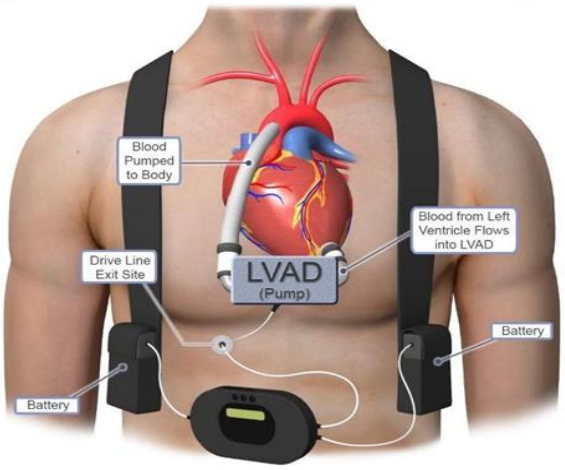

Figure 2.7 LVAD system [14]

- **Centrifugal pump:**

The Centrifugal pump is an assembly of three parts; 1) The Impeller, 2) The Spiral casing and 3) The Motor. The Impeller has a shape of a disc with blades arranged in regular manner giving rise to vanes. The Blades of the impeller are backward curved in order to provide least displacement to the blood flowing through the vanes. The inflow of the impeller is located at the center of circular disc along the axis of rotation. The inflow of the impeller is called as eye of the impeller. The centrifugal force of the rotating impeller pushes the fluid circumferentially and the fluid spirals out and discharges through the outlet. The figure 2.8 below, shows the volute of the centrifugal pump of Heart Ware HVAD.

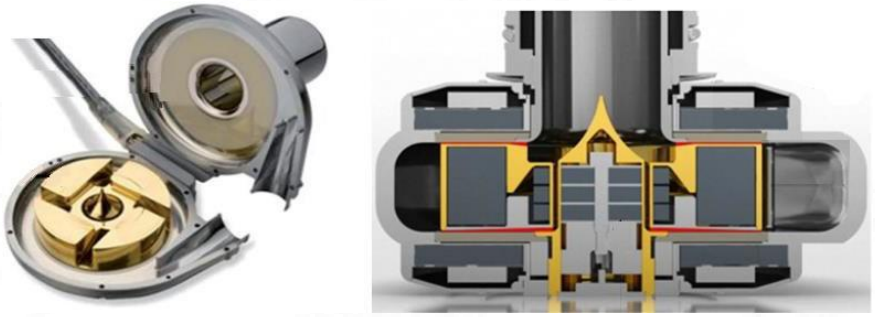

Figure 2.8 Volute and impeller set of centrifugal pump (Left) and magnetic levitation and hydrodynamic thrust (Right) of Heart Ware HVAD CF pump. [21]

The Motor of the pump comprises of the passive magnets attached in the inner part of rotor while the stator comprises of active electromagnets which are excited with the appropriate phase difference. That creates rotating magnetic field around the impeller causing the impeller to rotate in the same direction of field. The rotor uses magnetic levitation to maintain a certain clearance from the stationary stator as shown above in figure 2.8. The base of the impeller is kept from the stationary base by forming a thin layer of fluid creating a hydrodynamic thrust. This thin layer of fluid is generally blood.

- **System Controller:**

The main function of the system controller is to supply regulated power to the pump. However, the controller also regulates and monitors the pump functioning. It also Identifies alarm conditions and initiates hazard and advisory alarms in case of any power lag occurred due to low battery or any other system malfunction. Figure 2.9 features a controller of Heartmate III. The user interface of the LVAD controller displays following information however, it differs with controller to controller.

1) Pump Parameters (Flow, Speed, Power)
2) Status of Backup Battery Charge
3) Visual alarms with actionable instructions.

Modern controllers are provided with a backup battery is housed within the case. The other important function of controller is to carry out driveline diagnostic capability and records alarm data and device performance.

Figure 2.9 System Controller of LVAD HeartMate III. [Abbott Cardiovascular]

- **Power Module**

A power module is designed with the virtue of allowing patient to be mobile. The Module houses two batteries are connected to system controller. These batteries provide backup of 6-12 hours a pair. However, battery backup depends on the type of instrument used. Equipment can be carried in several different ways depending on the type of accessory. The figure 2.10 below shows the power module of Heartmate III. The Power Module (PM) provides AC mains electrical power to the HeartMate III LVAD system. In addition to powering the LVAD, the PM can simultaneously power the HeartMate Display Module or System Monitor. The PM power cord and patient cable first need to be attached before being power the system.

Figure 2.10 Power Module of LVAD HeartMate III. [Michigan Medicine]

- **Accessories**

The other components of LVAD are Inflow cannula which is inserted into the orifice made in the ventricle that draws blood into the impeller. Similarly, the Outflow Graft carries the discharged blood all the way into the ascending aorta. An additional strain relief is attached around the outflow graft to nullify any stress subjected to the graft. The Driveline or percutaneous driveline supplies the power from the controller to the pump piercing through the skin. To keep all the components in place while the patient is mobile, various accessories are

provided like belt attachment, travel bag or battery holster as shown in figure 2.11.

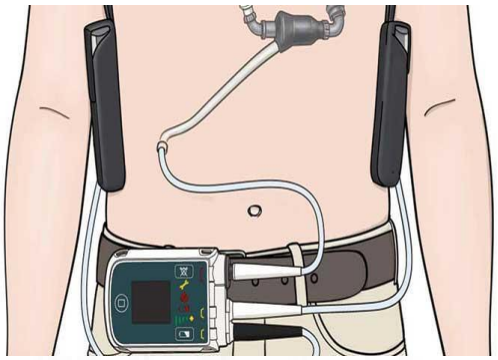

Figure 2.11 LVAD Holster Vest. [Michigan Medicine]

2.5 Classification of LVADs

As the requirement of advancement in the technology and the studies done before there exist a need of modification in the previous pulsatile design. This modification led to the development of CF devices. So based on the type of flow LVADs may be as pulsatile or continuous in nature Depending on the pump design and type of flow LVADs are classified as first generation, second generation and third generation type of devices. Examples of LVADs under this classification is given in table 2.3.

Table 2.3 Classification of LVAD

	First Generation	Second Generation	Third Generation
PUMP Design	Pulsatile Flow	Continuous Flow (Axial Pumps)	Continuous Flow (Centrifugal Pumps)
LVAD Types	HeartMate XVE	HeartMate II	HeartMate III

2.5.1 **First generation ventricular assist devices**

The first generation of LVADs are pulsatile devices because they have normal beats as like the normal human heart. Anatol Prinzing. et.al under the study, ‘Left ventricular assist devices—current state and perspectives’ [6] describes that ventricular assist devices are either pneumatically or electrically driven membrane pumps which generates pulsatile flow and having artificial heart valve at inlet and outlet. Some of the examples of first generation VADs are Thortec PVAD, XVE and Berlin Heart EXCOR.

During the evolution of LVADs, the basic principle used initially is that blood flows through an artificial chamber and then squeezed out to the rest of the body. The first version of LVAD that

approved by FDA in 1994 which was using air and external large machine for power. Electric version of that was approved in 1995. Both of the device was given the same name HeartMate and are collectively referred to as HeartMate I. This is because they both are from the same company, Thoratec. Later Another company Novacor also received FDA approval for LVAD. HeartMate I was used as BTT and it kept people alive for 18 months to two years after implantation.

Figure 2.12 below shows connection of patient to HeartMate I which is also known as XVE.

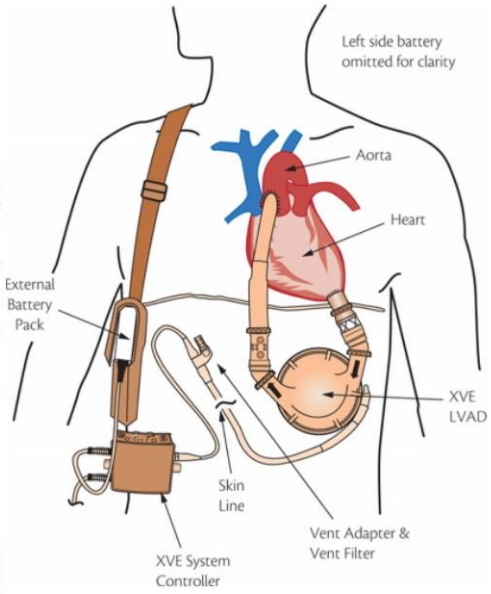

Figure 2.12 Patient connected to HeartMate I [St. Jude Medical, Inc.]

Due to population was increasing the number of heart patients were increasing and then people wondered that whether LVAD can be used more than bridge. After some modification, study was done on some patients and HeartMate became the first LVAD which was approved for the Destination Therapy. Then after some time modification had done and the pulsatile devices were replaced with continuous devices.

2.5.2 **Second Generation Left Ventricular Assist Devices**

Due to some modification needed in the first generation LVADs there came the concept of continuous flow devices. HeartMate II is the device which was invented under this category and this mechanism provided by the rotating screw. Blood comes into the chamber and twisted through a small device which was more comfortable than the previous one. It was examined from the various studies that longevity of the pump was more as compared to the HeartMate I. [6]

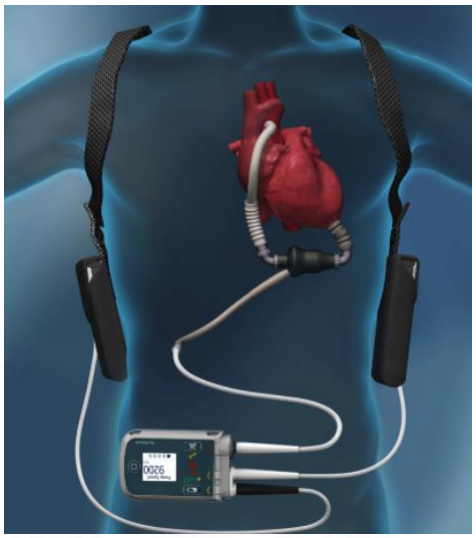

Figure 2.13 HeartMate II patients connected to LVAD [6]

Second generation devices were also needed some improvement due to having some complications after implantation. Later, concept of third generation devices was came which has discussed in the next section.

2.5.3 **Third generation Left Ventricular Assist Devices**

Due to some complications and problems associated with the second-generation devices there was needed some modification. Then the concept of electromagnetic devices came which was then called as third generation devices. It is based on centrifugal force and there are electromagnets which is spinning the blood. Heart ware HVAD is the device which is having a chamber with no mechanical bearing and since the device is small so it fits and attached to the apex of heart. Blood comes from the top and comes out at the right angle from the outflow pipe. In 2012, FDA approved this device for BTT and later after some time for destination therapy with the name Heart Ware HVAD. The inside view is shown below in the figure 2.14 (left). The device has hybrid passive magnetic bearing and hydrodynamic bearing (axial faces of the blades) to levitate the rotor. Later, HeartMate III which is having actively magnetically levitated rotor came in the market after approved by FDA. In the device Impeller and the magnets are axially spaced from one another. This device reduces blood shear stress. Heart Ware HVAD and HeartMate III is shown below in the figure 2.14.

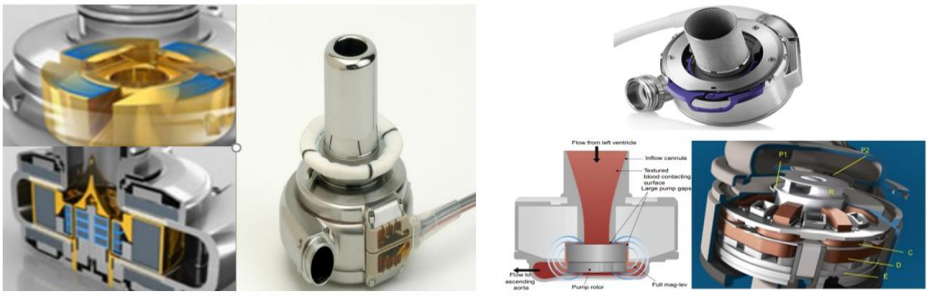

Figure 2.14 Heart Ware HVAD (Left)[8] and HeartMate III (Right) [8]

- **Advantage of non-contact bearing design:**
  - Low frictional wear
  - Reducing heat generation
  - Durability Increases
  - Washing of impeller (reduces risk of thrombus formation)
- **Bearing technology used in LVADs:**
  1. **Hydrodynamic Bearing:** Hydrodynamic bearing is a type of bearing in which separation between the impeller and the casing of pump is created by providing specially designed hydrodynamic pad features as a part of impeller geometry. There a hydrodynamic wedge of high-pressure fluid underneath the pad is created. Therefore, as impeller rotates hydrodynamic lift forces are generated under the hydrodynamic bearing features that will creates the separation between impeller and casing of the pump.
  2. **Magnetic Bearings:** A magnetic bearing is a type of bearing that supports the load using magnetic levitation. There are two types of magnetic bearings, Active which require electromagnets and passive which require permanent magnets. Magnetic bearings make it easier to reduce area of high shear stress (which leads to red blood cell damage) and flow stagnation (which reduces blood clotting) in blood pumps.
- **Material Used in LVADs:**

  The impellers of the axial and centrifugal blood pump are mostly made of titanium and ceramic. The inner surface of the pump housing coated with segmented polyurethane and the impeller are sprayed with a coating except for the top (shroud) surfaces of blades. The shaft and bearing are usually made of stainless steel or titanium with varying properties (hemolytic) depending on the design of the bearing. The stator was molded with epoxy resin to prevent infiltration of water. Shaft and bearing surfaces are coated with 2-polymer methacryloyloxyethyl phosphorylcholine (MPC) to make the surface of the shaft sufficient enough to avoid thrombus formation. To prevent the risk of thrombosis careful treatment of the anti-thrombogenic material coating is necessary. [16]

  On the motor side, a layer of (Teflon) polymer is mounted between the casing and impeller to reduce friction. Transparent acrylic used sometimes for impeller wall. The pump materials in contact with the blood are primarily Polycarbonate (PC), and the pivot bearing is a combination of stainless steel (SUS) ball and a receptacle of ultra-high-molecular-weight polyethylene (UHMWPE).[16]

2.6 Major Complications Related to LVADS

1. **Right Ventricle (RV) Failure:** Unloading of left ventricle after LVAD implantation results in septal shifts. That increases the pre-load on right ventricle and which leads to decreases the contractility and function of right ventricle. RV failure can be determined with the help of echocardiography after post-operation.
2. **Gastrointestinal Bleeding:** This type of complication can be seen mostly in CF LVADs. These patients are systematically anticoagulated with the warfarin. The most common cause for this complication is arteriovenous malfunctions or angiodysplasia. To reduce it at some level running LVADs can be operated at low RPMs.
3. **Pump Thrombosis and Strokes:** This type of complication can be seen in II and III generations LVADs. It was founded that this complication can occur after three- and six-months implantation of LVADs
4. **Infection:** It can occur anywhere like at cannula insertions at the apex of LV and to the ascending aorta, driveline through which LVAD is connected to power source through skin. This can be managed by debridement of infected tissue.
5. **Ventricular Arrythmias:** This type of complication generally occurred at early post-operative period. Common cause of this is suction events where inflow cannula sucks too much blood bringing the cannula to oppose the septum which results unloading of LV and that can lead to collapsing. Remedy for this is to reduce the LVAD flow rate which will lead to greater LV filling.
6. **Hypertension:** This type of complications also occurred in CF LVADs because they do not have systolic or diastolic pressure. Mean arterial pressure (MAP) is accessed with the doppler. If MAP is more than 90mmHg then there can be chance of hypertension and stroke risk increases in such case. A good management for this complication to use conventional agents like ACE inhibitors, B- Blockers etc. Hydralazine can be used for rapidly effectiveness and make the MAP in range 60-70 mmHg.
7. **Pump-Optimization:** Optimal speed should be identified with the help of echocardiography and pump should be optimized at different RPMs.

2.7 Chitra LVAD

Sree Chitra Tirunal Institute for Medical Sciences and Technology (SCTIMST), Trivandrum, under the Department of Science and Technology Govt of India. They are one of the pioneers in medical devices development. SCTIMST took responsibility for developing a Left Ventricle Assist

Device (LVAD) which is named as Chitra LVAD as shown below in the figure 2.15. The device has both hydrodynamic and magnetic bearing. Magnetic bearing has been used to levitate the rotor. The Device has centrifugal pump which has made for implanted in the body at apex of the left ventricle of the heart. The Centrifugal pump is an assembly of three parts; 1) The Impeller, 2) The Spiral casing and 3) The Motor. Other components include inflow cannula, outflow graft, driveline coming out from the abdomen, System Controller, Power Sources (Power module, Battery), Percutaneous lead, Power cord and other required Accessories.

Figure 2.15 Chitra LVAD [17]

- **Motor used in Chitra LVAD:**

Chitra LVAD has BLDC motor which is controlled by BLDC controller attached in LVAD controller. Speed of the rotor is maintained through the hall sensor attached in the motor which provide the feedback pulse to LVAD controller and through which speed is controlled. The BLDC motor is star connected and able to produce torque of 10m-Nm approximately when 1A of current is delivered.

The major difference between brushed and brushless DC motor is that the BLDC motor have its winding built on the stator and permanent magnets on the rotor. The commutation is done electronically not via brushes which eliminated the heat loss due to brushes.

BLDC motor have several advantages:

- Better speed vs torque characteristics
- High efficiency
- Long operating life due to due to lack of friction and electrical losses

- Better thermal handling capacity
- Effective heat dissipation
- Better dynamic response
- Noiseless operation

2.8 Electrical Machine Concepts

This section provides the concept for computation of BLDC motor parameters in Chitra LVAD using experimental techniques that helped in the efficiency computation of the motor used in the Chitra LVAD. Basics of torque, various types of electrical machines and their governinig equations, characteristics are described.

- **Torque:**
  - Torque is defined as the measure of the force that can cause any object to rotate about its axis. It is also called as **moment, rotational force, moment of force or turning effect** according to the field of study.
  - If a force 'F' is applied on a circular body having radius 'r' then the torque will be equals to: $\tau = F \times r = Fr\sin\theta$

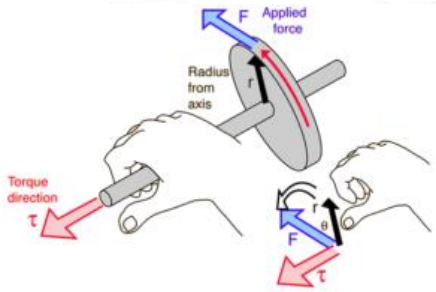

Figure 2.16 Measuring of Torque [18]

- **Electrical Machines:**
  - An electric machine is a device which converts electrical energy into mechanical energy or vice versa.
  - The basics of DC machines is discussed so to understand the methodology used for electrical efficiency computation for Chitra LVAD.
  - Construction of a generator and a motor is similar only the input and the output energy have difference.
  - Generator have mechanical energy is the input energy and electrical energy as the output energy. while motor have electrical energy is the input energy and mechanical energy is

the output energy.

- Electrical machines are broadly classified as shown below in the flow chart:

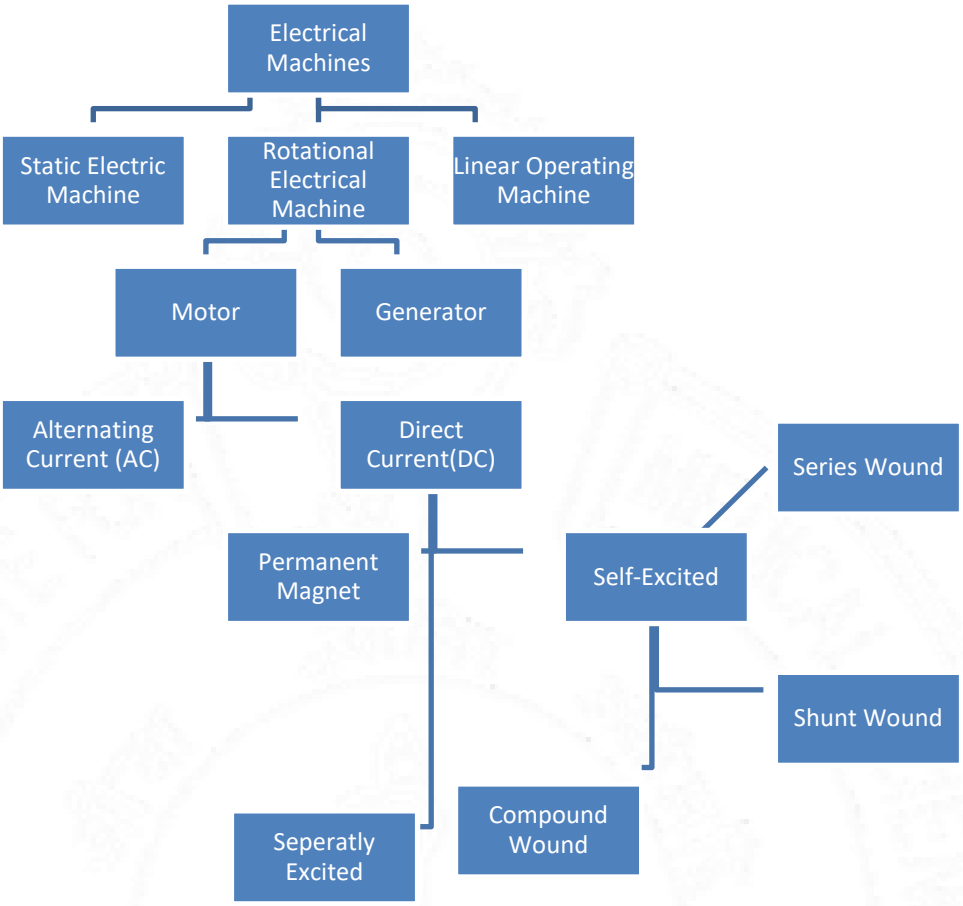

Figure 2.17 Classification of Electrical Machines

Before going further discussion about the concept used for torque computation for Chitra LVAD basic principles behind the concept are discussed. EMF equation of a DC machine, Torque equation of a DC motor, characteristics of a DC motor are explained to understand the torque speed curve of the motor that is used in Chitra LVAD.

EMF Equation of a DC Machine:

Assume that there is a DC machine which is having:

- Flux per pole = φ wb
- Total number of conductors = Z
- Revolution per minute = N

- Number of Poles = P
- Number of Parallel Path = A (for lap winding A=p & for wave winding A=2)

In one parallel path,

Flux linked with one revolution made by one conductor present in one parallel path = P Φ

Time taken by one conductor for one revolution = $\frac{60}{N}$

Emf induced in one conductor in one revolution = $E = \frac{\text{Flux linked in one revolution}}{\text{Time taken in one revolution}} = \frac{P\varphi}{60/N} = \frac{P\varphi N}{60}$

Number of conductors in one parallel path = $\frac{\text{Total number of conductors}}{\text{Number of parallel paths}} = \frac{Z}{A}$

Therefore, Emf induced in conductors in one parallel path will be =

$$\text{Emf induced in one conductor in one revolution} \times \text{Number of conductors in one parallel path} = \frac{P\varphi N}{60} \times \frac{Z}{A} = \frac{\varphi ZNP}{60} \ldots (1)$$

In case of a DC generator, it is called as a generated Emf (E_g) and in case of a DC motor it is called as a Back Emf (E_b).

After computing equation of back Emf for DC motors next is to understand dependency of torque on armature current so that can help to relate torque and speed via armature current. In all this procedure back Emf play a very significant role, that has been discussed later in this chapter.

Torque equation of DC motor:

Torque depends on constructional and operational parameters of a DC motor (here torque has been considered as armature torque since rotor is rotating and having armature inside it).

Assume a motor which is running at angular velocity ω rad/sec in clockwise direction and a force F Newtons (N) is applied on it as shown in the figure below.

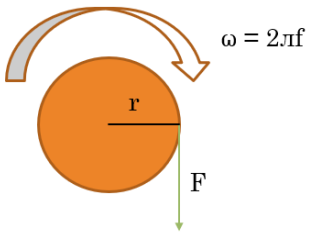

Figure 2.18 Rotating Structure (Rotor)

Where ω is the angular velocity and it is equal to,

$$\omega = 2\pi f, f = \text{frequency (Hz)}$$

$$\text{where, } f = \frac{1}{T} \text{ where } T = \text{Time Period} = \frac{60}{N}, N = \text{Revolution per min}$$

$$\text{Therefore, } f = \frac{N}{60}$$

Now, the angular velocity ω is,

$$\omega = \frac{2\pi N}{60}$$

As already known that torque produced in the given machine can be given as

$$\tau = F \times r \text{ where } r = \text{radius from the center in meters}$$

In other words, $\tau = F \times$ distance covered $= F \times 2\pi r$, where circumference $= 2\pi r$

Mechanical power developed by the motor is given as,

$$P_{out} = \frac{\text{Work done}}{\text{Time}} = \frac{F \times 2\pi r}{60/N} = \frac{F \times 2\pi r \times N}{60}$$

$$\text{Since armature torque } T_a = F \times r$$

Therefore, the mechanical output power of DC motor will be,

$$P_{out} = \frac{2 \times \pi \times N \times \tau_a}{60}$$

Now, the Electrical input power of DC machine can be given as

By applying Kirchhoff's Voltage Law (KVL) in the figure shown we get,

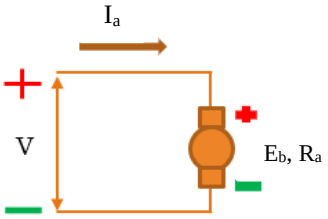

Figure 2.19 General circuit for a DC machine

$$-V + I_a R_a + E_b = 0$$

$$V = I_a R_a + E_b \ldots\ldots\ldots\ldots\ldots\ldots (2)$$

Multiplying I_a both the sides,

$$VI_a = {I_a}^2 R_a + E_b I_a$$

Consider the ideal condition so neglecting losses $({I_a}^2 R_a)$ then,

$$vI_a = E_b I_a$$

$$\text{Therefore, Electrical input power will be, } P_{in} = VI_a = E_b I_a$$

For ideal case,

$$P_{in} = P_{out}$$

$$E_b I_a = \frac{2 \times \pi \times N \times \tau_a}{60}$$

$$\text{Where, } E_b = \text{Back Emf} = \frac{\varphi ZNP}{60}, \text{from equatiton (1).}$$

By putting all the values and rearranging the above equation,

$$\tau_a = \frac{\varphi Z P I_a}{2\pi A}$$

Therefore, $\tau_a \propto \varphi I_a$ ..... (3) , Since all other things are fixed or constant .

Significance of Back Emf:

As mentioned in equation 2 , $V - E_b = I_a R_a$

$$\text{So, } I_a = \frac{(V - E_b)}{R_a} \text{ ..... (4)}$$

Since R_a and V are fixed or constant therefore, $I_a \propto E_b$

Consider three cases;

Case I: When there is no load applied on DC machine,

Speed will increase if no load will be there that will lead to cut more magnetic field lines and more flux linkage will occur. Because of that induced emf (which is back emf, E_b) will increase and from equation 4, (V-E_b) will decrease so armature current (I_a) will decreases and as from equation 3, τ_a will decrease.

Case II: When DC machine is suddenly loaded,

Speed will decrease that will lead to cut less magnetic field lines and less flux linkage will occur. Because of that induced emf (which is back emf, E_b) will decrease and from equation 4, (V-E_b) will increase so armature current (I_a) will increase and as from equation 3, τ_a will increase.

Case III: When load gradually decreases,

Speed will increase if load will decrease gradually and that will lead to cut more magnetic field lines and more flux linkage will occur. Because of that induced emf (which is back emf, E_b) will increase and from equation 4, (V-E_b) will decrease so armature current (I_a) will decreases and as from equation 3, τ_a will decrease.

From the above three cases it has been proved that DC machine behaves as a self-regulating machine. In case of DC motor, it can draw as much as armature current as is sufficient to develop the torque required by the load.

Now, after understanding the significance of armature current and back emf on torque of a DC motor. Next is to variation of torque with the speed of a DC motor. For that first thing is to understand some characteristics of DC motor (for e.g., here series and shunt dc motors have been taken to made one to understand the characteristics of DC motors).

Characteristics of a DC motor:

A comparison between series and shunt DC motor has been provided to understand the torque and

speed characteristics of DC motor.

Generally, for any DC motor we consider 3 types of main characteristics,

1. Torque Vs Armature Current
2. Speed Vs Armature Current
3. Speed Vs Torque

For DC shunt motor: In DC shunt motor field windings are attached in parallel. Voltage is always same in parallel. Shunt field winding resistance is fixed so current flowing through field windings will be same always and that will develop a constant flux. Therefore, DC shunt motors are also known as constant flux motors.

from equation (3), $\tau_a \propto \varphi I_a$, for DC shunt motors flux linkage will be constant so $\tau_a \propto I_a$

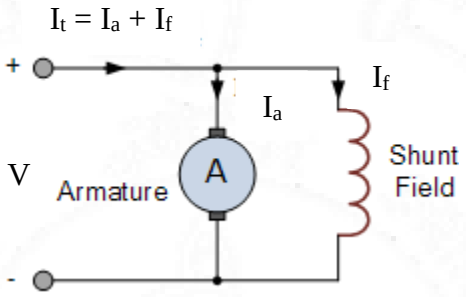

Figure 2.20 General circuit diagram for DC shunt motor [20]

1) Torque Vs Armature Current: If load will increase that will increase the armature current and torque will increase.

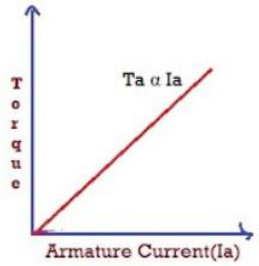

Figure 2.21 Torque vs Armature Current for DC shunt motor

2) Speed Vs Armature Current: for DC motor speed is related to induced emf as,

$$N \propto \frac{E_b}{\varphi} \frac{\propto (V - I_a R_a)}{\varphi}$$

So, if load increases that will lead to increase the armature current because of that $(V - I_a R_a)$ decreases and that will lead to decrease the speed as flux is already constant.

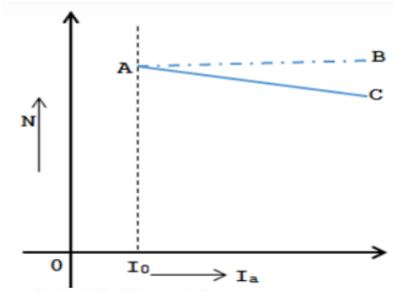

Figure 2.22 Speed Vs Armature Current for DC shunt motor

3) Speed Vs Torque: Torque is directly proportional to the armature current so for DC shunt motor speed Vs torque will related as,

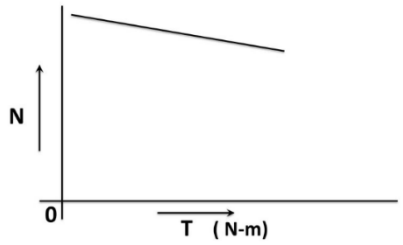

Figure 2.23 Speed Vs Torque for DC shunt motor

For DC Series motor: In DC series motor, field windings are attached in series. Voltage is not same in series but current will be same. Shunt field winding resistance is fixed so current flowing through field windings will not be same always and that will develop a variable flux. Therefore, DC series motor are also known as variable flux motor.

Since we know from equation (3), $\tau_a \propto \varphi I_a$, for DC series motor flux linkage will be not be constant,

$$So, \tau_a \propto \varphi I_a$$

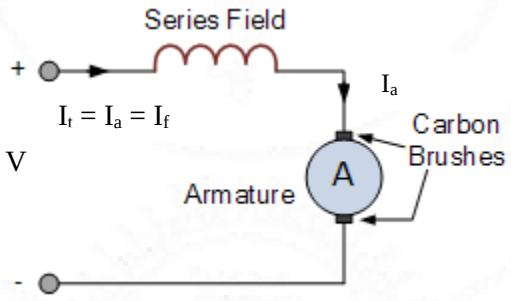

Figure 2.24 General Circuit diagram for a DC series motor. [20]

1) Torque Vs Armature Current: If load will increase that will increase the armature current. Due to increase in armature current winding current also increases as both are in series. Because of that flux linkage will increase but at a certain level flux will become saturate and then torque will only depend on armature current.

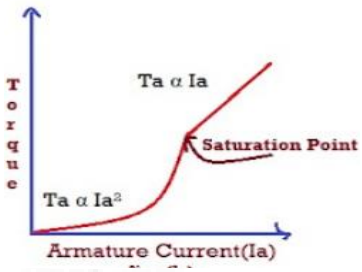

Figure 2.25 Torque Vs Armature Current for DC series motor

2) Speed Vs Armature Current: For DC motor speed is related to induced emf as,

$$N \propto \frac{E_b}{\varphi} \propto \frac{(V - I_a R_a)}{\varphi}$$

So, if load increases that will lead to increase the armature current. Because of that $(V - I_a R_a)$ decreases. I_f will also increase that will lead to decrease the speed more because flux is also increasing.

The graph between the speed and armature current has been shown below in the figure 2.26 where speed is decreases with increase in current.

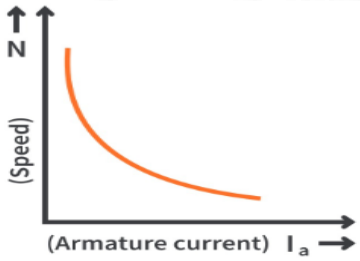

Figure 2.26 Speed Vs Current for DC series motor

3) Speed Vs Torque: As Torque is directly proportional to the armature current. For DC series motor speed and torque are related as; first it will decrease by two factors one is due to increase in the armature current and second is due to increase in flux linkage due to increase in field winding current. But after a saturation point flux cannot increase more and then torque will depend on armature current only and similarly speed also behaves therefore the relationship between speed and torque has been shown below in the figure.

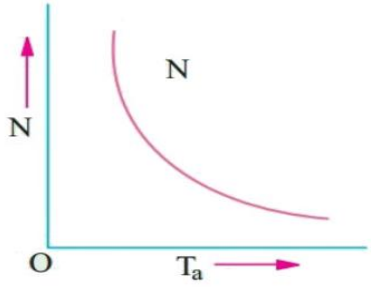

Figure 2.27 Speed Vs Torque for a DC series motor

The above concepts have been helped to obtained the results and also helped to understand the characteristic curve of BLDC motor obtained experimentally.

Chapter III

Project Objectives

This chapter provides the objective of the study which is based on the fact that efficiency of the pump is one of the major parameters which have a great impact on pump performance of Chitra LVAD. LVAD is a centrifugal pump which is having two parts mechanical and electrical motor. Impeller and the casing come under mechanical part and the motor is the electrical part of the pump. Most of the LVADs are having Brushless Direct Current (BLDC) motor because of their certain advantages such as high efficiency and good speed and torque characteristics. BLDC motor are also called as electronically commutated motor because in case of BLDC motor electronically speed controller is used as a commutator.

One of the major factors that effects the efficiency of the pump is BLDC motor used in the pump. The overall efficiency of the Chitra LVAD is a combination of the hydraulic as well as electrical efficiency of the motor. It is thus imperative to study the efficiency of the BLDC motor to have a pump with good performance parameters that lead to have a better durability and the function of the device. As shown below in block diagram, the input is electrical power and the output is hydraulic power. Electrical power supply is given to Chitra LVAD controller which operated the BLDC motor and impeller starts rotating. So, the electrical power is converted into the mechanical power. Hall sensor are provided with motor and they are providing feedback to the controller to control the speed. Impeller then drive the fluid and that mechanical power converts to hydraulic power. So, as first electrical power is converted to mechanical power and then mechanical power converted to hydraulic power. So, for computation of overall efficiency there will be two factors i.e., electrical efficiency which is ratio of mechanical power to electrical power and hydraulic efficiency which is ratio of hydraulic power to mechanical power. If overall efficiency is known and electrical efficiency is computed, hydraulic efficiency of the pump can be computed easily with arithmetic operation as given below.

The following block diagram illustrated to understand the objective of the project:

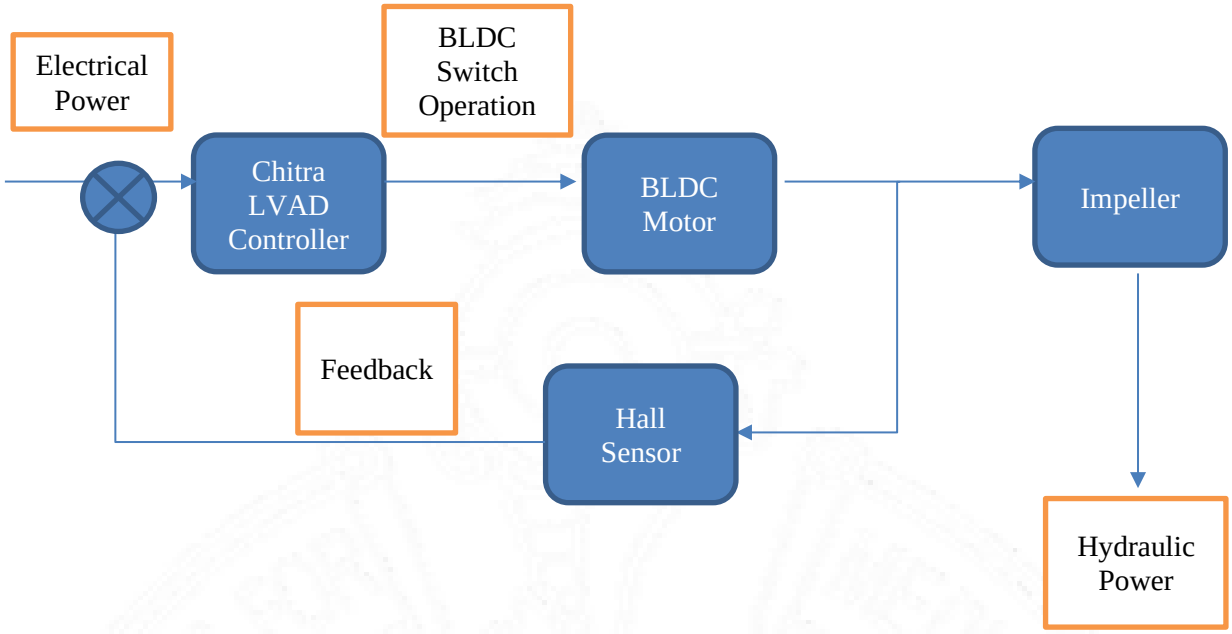

Efficiency of motor included the hydraulic as well as electrical efficiency:

$$\text{Hydraulic Efficiency} = \frac{\text{Hydraulic Power}}{\text{Mechanical Power}} \ldots\ldots\ldots (1)$$

$$\text{Electrical Efficiency} = \frac{\text{Mechanical Power}}{\text{Electrical Power}} \ldots\ldots\ldots (2)$$

$$\text{Therefore, Overall Efficiency} = \text{Hydraulic Efficiency} \times \text{Electrical Efficiency} \ldots\ldots\ldots (3)$$

$$\text{Overall Efficiency} = \frac{\text{Hydraulic Power}}{\text{Electrical Power}} \ldots\ldots\ldots\ldots (4)$$

The objective of the project is to compute the electrical efficiency of the BLDC motor used in the Chitra LVAD. To achieve the primary objective project has been sub-divided into multiple secondary objectives such as:

1. Prepare a CFD model to obtain a H-Q curve of the pump used in Chitra LVAD.
2. Compare the obtained H-Q Curve with the standard experimental hydraulic performance H-Q curve of Chitra LVAD.
3. To Compute the torque using CFD model at 2500 RPM using simulation.
4. Develop an experimental set-up for computation of torque of BLDC motor used in Chitra LVAD.

5. Compare the torque value obtained from the experiment setup with conventional measurement technique for computation of torque.
6. Compare the Torque obtained from simulation and experimental analysis.
7. Compute the Electrical Efficiency of BLDC motor used in Chitra LVAD.
8. Plot Efficiency Vs Speed Characteristic of BLDC motor used in Chitra LVAD.

Chapter IV

Torque Computation using Computational Fluid Dynamics

This chapter discusses the basic working principle of Computational Fluid Dynamics (CFD) and the process used for computation of torque, H(head)-Q(flow) curve from the simulations. For the same, a CAD model was developed using CREO parametric software and the simulations were performed with the help of Ansys Workbench software using CFD concepts.

4.1 Computational Fluid Dynamics (CFD)

CFD is a branch of fluid mechanics which uses data structures and numerical analysis to analyze and solve many problems which involves fluid flows. Computers are used to do the calculations and perform the simulations with specified boundary conditions. For achieving better solutions high-speed supercomputers are used. These supercomputers are used generally to solve complex problems which are largest and require good results with good accuracy. CFD can be used in many engineering fields to solve wide range of problems such as aerodynamics and aerospace analysis, hypersonic, weather simulation, environmental engineering and natural science, heat transfer, biological engineering, visual effects of films and games, combustion analysis etc. Numerical methods are used to convert the partial differential equations into the algebraic set of equations in CFD analysis.[19]

CFD uses a group of computational methodologies which are used to solve equations of different fluid flow dynamics. For a specific application there is a critical step which can be used to decide which set of equations and assumptions are to be used for the simulations. Flow equations that are solved using CFD are listed and discussed below:

- Conservation laws equations: These are the most fundamental equations that are used in the CFD. For a single-phase, single-species and compressible flow **conservation of mass, conservation of linear momentum and conservation of energy can** be considered.[19]
- Continuum conservation laws: Start with the conservation laws and assumes that there is a continuum medium, the resulting equations are unclosed and for solving it there needs further equations such as:
    - Constitutive relationships for the viscous stress tensor
    - Constitutive relationship for the diffusive heat flux
    - Equation of State (EOS)
    - Caloric equation of state relating temperature to enthalpy and internal energy

- Compressible Navier-Stokes Equations (C-NS): Start with the continuum conservation laws, assume there is a Newtonian viscous stress tensor. C-NS can be augmented with the EOS and caloric EOS to have a closed system of equations.[19]
- Incompressible Navier-Stokes Equations (I-NS): Start with the C-NS assume that the density is constant everywhere or another way is to say MACH number is very small and the temperature difference is also very small in the fluid. So, mass and momentum conservation equations are decoupled from energy conservation equation so only needs to solve two equations.[19]
- Compressible Euler equations, weakly compressible Navier- Stokes equations, Boussinesq equations, compressible Reynolds-averaged Navier-Stokes equations, ideal flow equations, linearized compressible Euler equations, sound wave or acoustic wave equations, shallow water equations, boundary layer equations, Bernoulli equations, steady Bernoulli equation, Stokes-flow or creeping flow equations, two dimensional channel flow and one dimensional Euler equation, Fanno-flow and Rayleigh flow equations are also can be used in the CFD for calculation many solutions for different applications of fluid dynamics.[19]

General form of Navier stokes equations that are used in CFD for solving a fluid flow problem,[9]:

$$\text{Mass: } \frac{\partial \rho}{\partial t} + \text{div}\,(\rho u) = 0$$

$$\text{x-momentum: } \frac{\partial(\rho u)}{\partial t} + \text{div}\,(\rho u u) = -\frac{\partial p}{\partial x} + \text{div}(\mu\ \text{grad}\ u) + S_{M_x}$$

$$\text{y-momentum: } \frac{\partial(\rho v)}{\partial t} + \text{div}\,(\rho v u) = -\frac{\partial p}{\partial y} + \text{div}(\mu\ \text{grad}\ v) + S_{M_y}$$

$$\text{z-momentum: } \frac{\partial(\rho w)}{\partial t} + \text{div}\,(\rho w u) = -\frac{\partial p}{\partial z} + \text{div}(\mu\ \text{grad}\ w) + S_{M_z}$$

$$\text{Internal Energy: } \frac{\partial(\rho i)}{\partial t} + \text{div}\,(\rho i u) = -\rho\,\text{div}(u) + \text{div}(k\ \text{grad}\ T) + \Phi + S_i$$

Equations of state: $p = p(\rho, T)$ and $i = p(\rho, T)$

e.g., for perfect gas: $p = \rho RT$ and $i = C_v T$

General form of governing equation can be written in compact form as;

$$\frac{\partial(\rho C \emptyset)}{\partial t} + \Delta \cdot \overrightarrow{a_\emptyset} = \nabla \cdot \vec{d}_\emptyset + S_\emptyset$$

$$\underbrace{\frac{\partial(\rho C \emptyset)}{\partial t}}_{\text{Unsteady}} + \underbrace{\frac{\partial(\rho u c \emptyset)}{\partial x} + \frac{\partial(\rho c v \emptyset)}{\partial y}}_{\text{Advection}} = \underbrace{r_\emptyset \left[\left(\frac{\partial^2 \emptyset}{\partial X^2}\right) + \left(\frac{\partial^2 \emptyset}{\partial Y^2}\right)\right]}_{\text{Diffusion}} + \underbrace{S_\emptyset}_{\text{Source}}$$

Numerical solution procedure:

CFD is a science which is known as of predicting fluid flows, heat, chemical reactions, mass transfer and other related phenomenon by solving the set of governing equations numerically. Generally, CFD works based on the conservative methods such as Finite Difference Method (FDM), Finite Element Method (FEM), Finite Volume Method (FVM). FDM is the oldest one and in now days most commonly used methods are FEM and FVM for which process is as shown below in the block diagram.

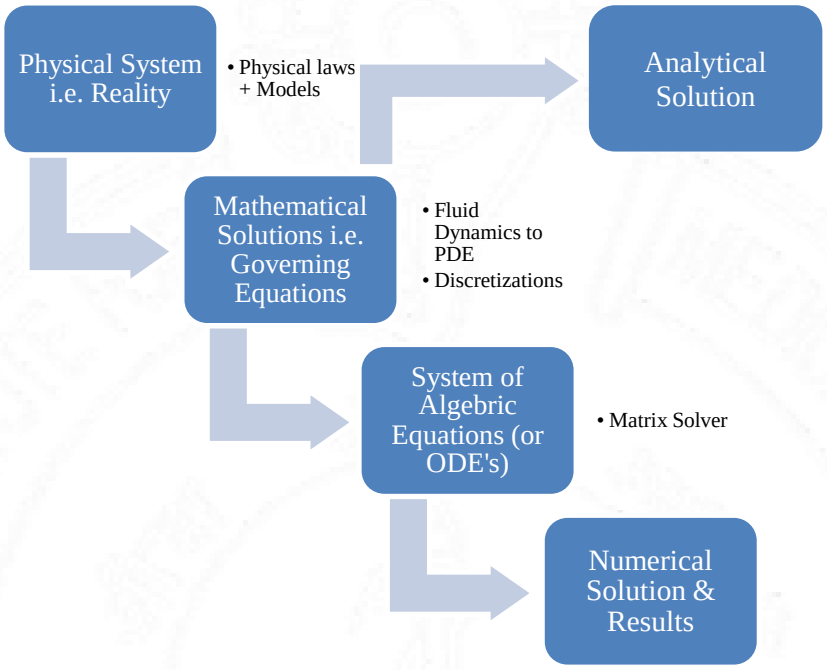

Figure 4.1 Work Process of CFD [9]

Steps for CFD Modeling's:

- Pre- Processing: It consists of making geometry and doing meshing.
- Solver: It consist of making setup for the simulation and adding solution criteria.
- Post- Processing: It is used to visualize the results.

Commonly used software's for CFD simulations are ANSYS, Autodesk CFD, Open Foam etc.

Now, after getting a broad picture of the computational flow dynamics next torque computation by using CFD is discussed. CFD approach was used to calculate the torque for Chitra LVAD and compared with the experimental results obtained at different conditions (such as boundary conditions, cell-zone conditions, method etc.,) were used and applied for computation of torque using CFD simulations.

4.2 Methodology used for calculation of torque using CFD.

- **Step 1**: **Geometry operations has performed using Ansys Workbench 18.2.**
    - Open the ANSYS Workbench 18.2. Click from the left mouse button on Start Menu and search their Workbench 18.2.

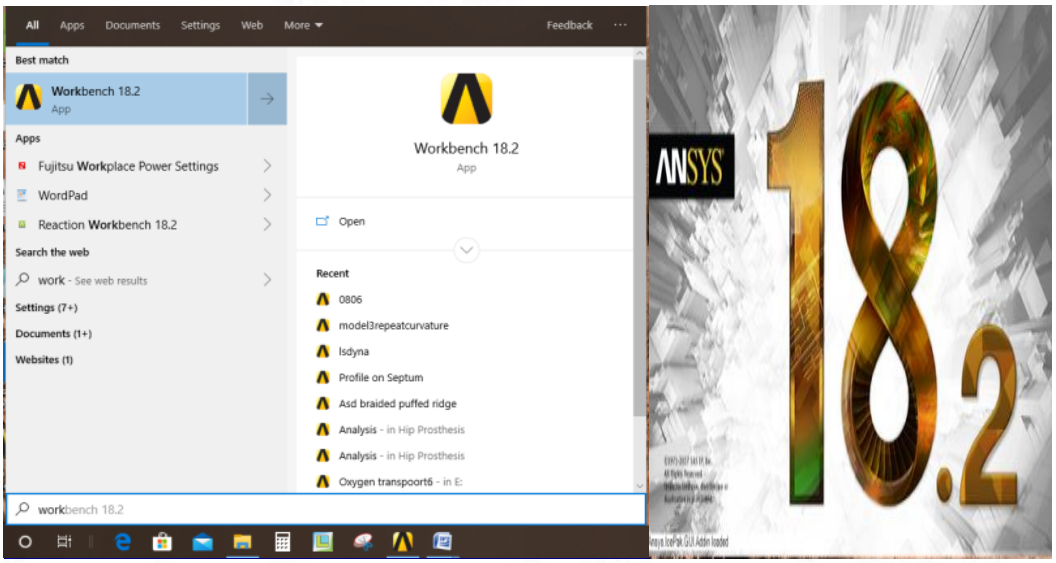

    - **Double Left Click** on **fluent flow (fluent)** mention at the left side of the screen in Analysis System Section under **Toolbox**. Open the fluent and then imported the geometry of the Chitra LVAD pump.

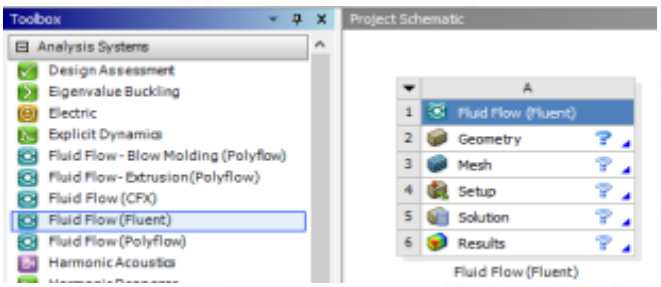

    - After fluent flow (fluent) selection Right Click on the Geometry and open New Space claim Geometry for making new geometry. Geometry was already available for Chitra LVAD, so just double click from the left mouse button and selected geometry in import geometry section.

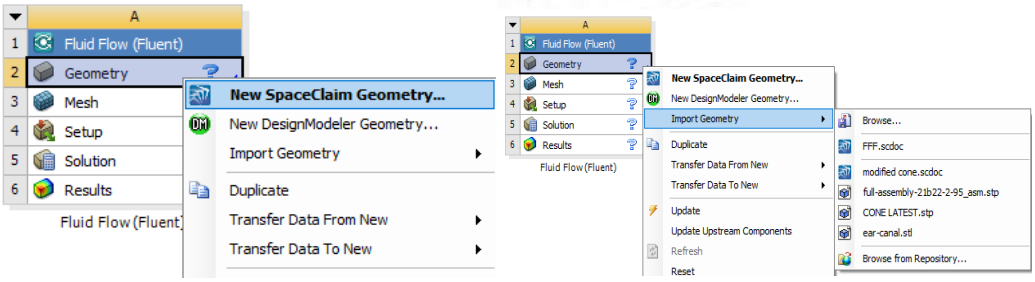

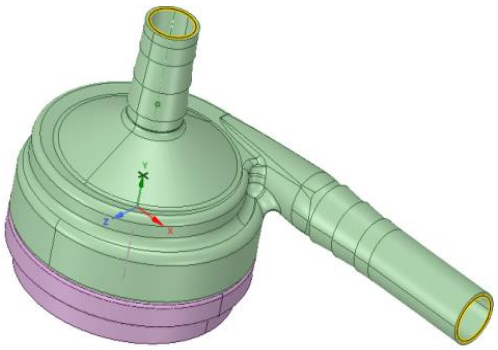

- Next, since geometry has imported so directly extracted the volume by select the option **Volume Extraction.** Select the **Prepare** menu and then go to the **Analysis** section and selected **Volume Extract**. After selecting volume extract then left click on **Select Edges** and select the edges of the shape where volume extraction needed.

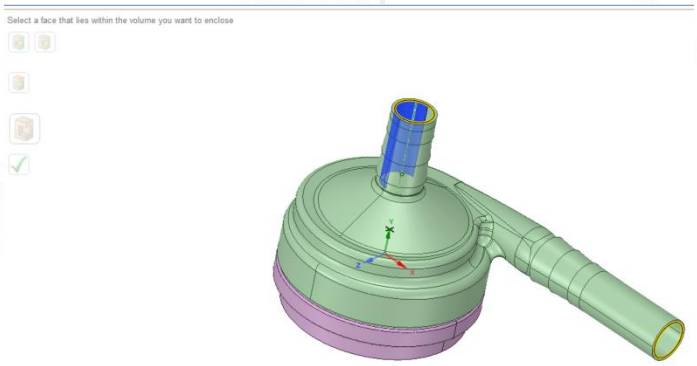

- After, Volume Extraction to see the extracted volume, go to the structure window on left side, there right click on solid and then by left click on Suppress for Physics that were suppress all the solid parts of the geometry.

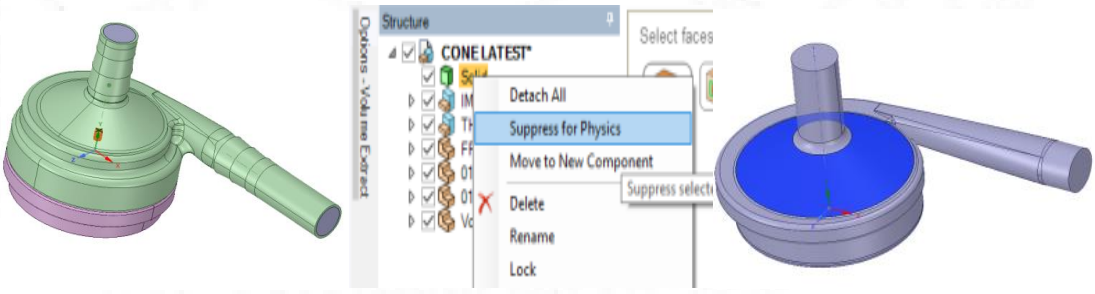

- A rotor surface has created around impeller to provide the rotational mechanism to the fluid. For that purpose, first made view as a section view by going to the Section Mode and then made an envelope around the impeller by selecting line under Sketch menu. First, offset was created and then applied pull option with using

option rotate along the central axis and that has rotated with the impeller as shown. By using split tool, separated the full fluid volume as two different volumes named as stator and rotor.

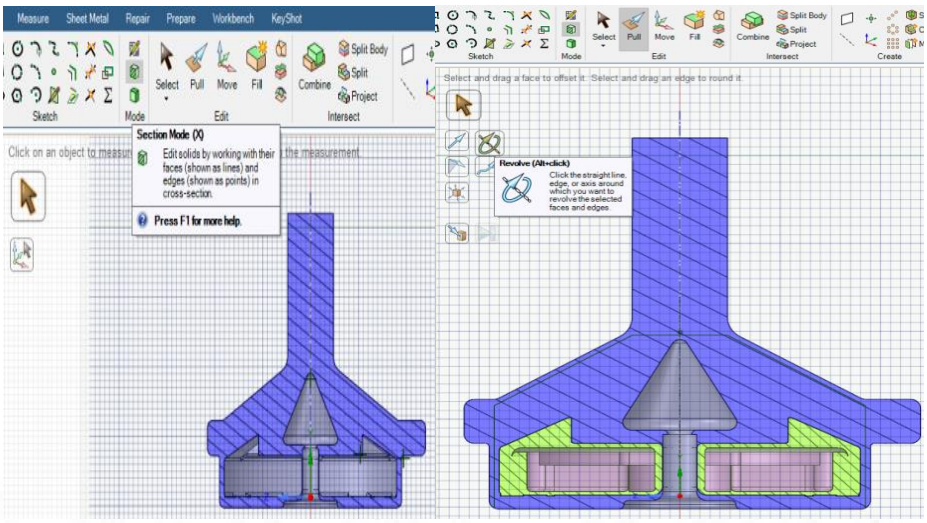

- Then Performed combine operations to separate the rotor and stator volume from extracted parts.

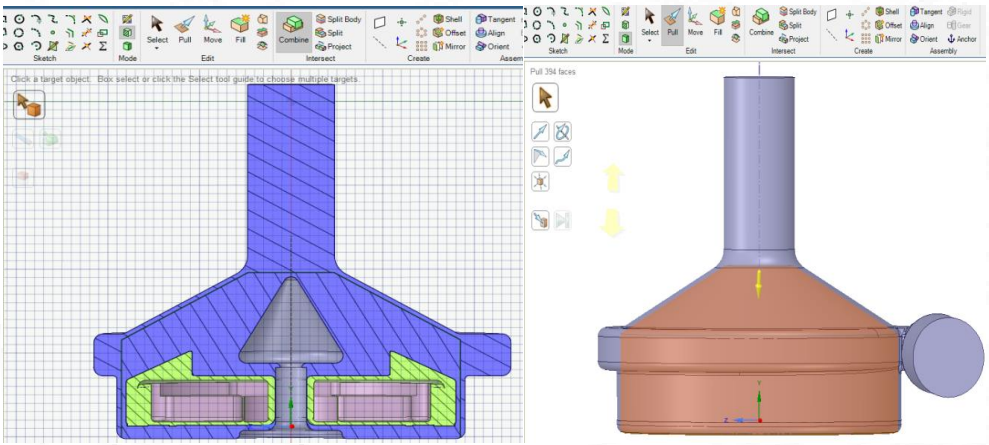

- After geometry was prepared all unwanted portions were suppressed. Then closed the Space claim module and then go to meshing.

- **Step 2: Generate Mesh**
  - Double Left Click on **fluent flow (fluent)** mention at the left side of the screen in **Analysis System** Section under **Toolbox** right click on **Mesh** then Left click on **Edit.**

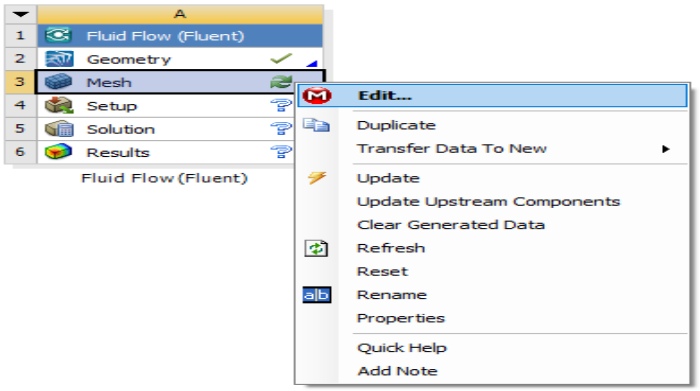

- Inserted a coordinate system that has shown below to specify the coordinate for particular location that will provide the frame of motion to the rotating surface.

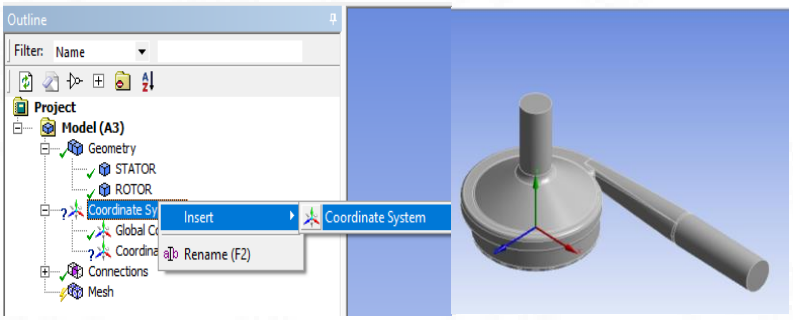

Details of "Coordinate System"	
Definition	
Type	Cartesian
Coordinate System	Program Controlled
Suppressed	No
Origin	
Define By	Global Coordinates
Origin X	0. mm
Origin Y	3.5 mm
Origin Z	0. mm
Location	Click to Change
Principal Axis	
Axis	X
Define By	Global X Axis
Orientation About Principal Axis	
Axis	Y
Define By	Default
Directional Vectors	
Transformations	

- Go to **Outline** window on the left side of the screen and right click on mesh then select Insert and then left click on Sizing.

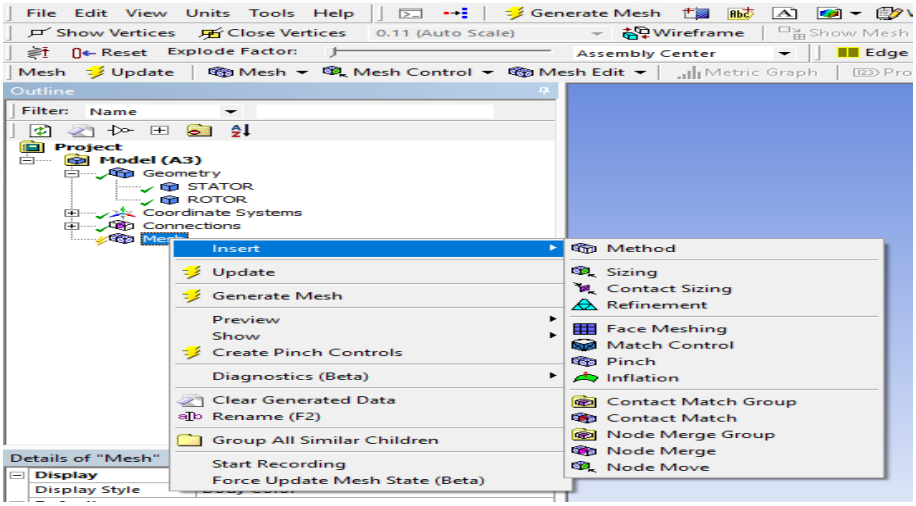

- Go to upper menu from their select **Body** option (or Ctrl+B) and select the body required.
    - Go to the left side of the window screen and Click on the Apply geometry which is in the **Details of Sizing** Section.

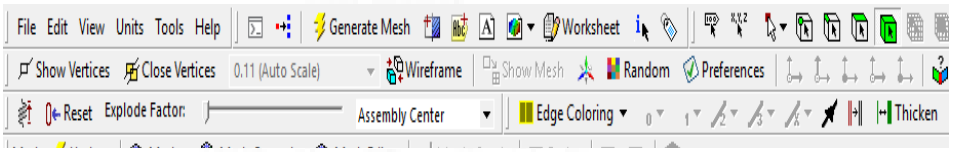

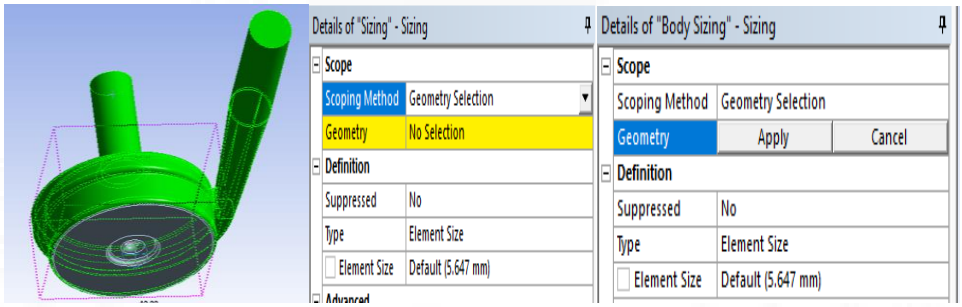

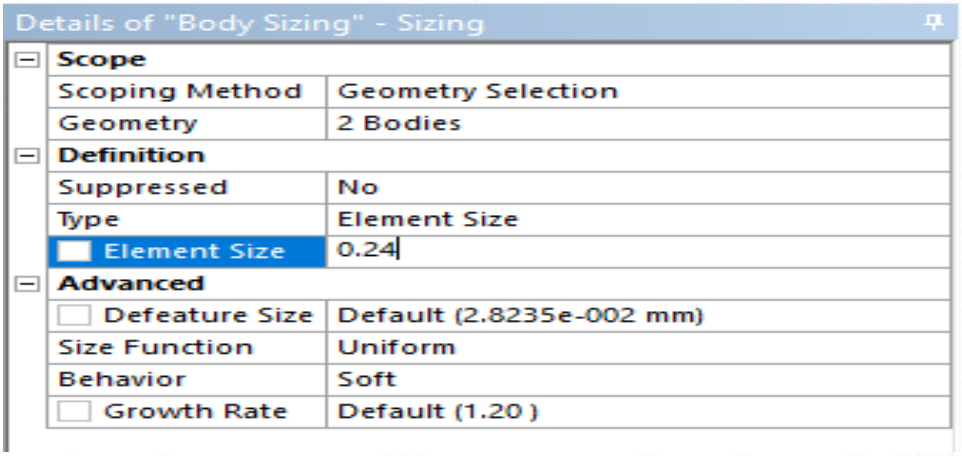

- Inserted the Contact Sizing and element size in the contact sizing.

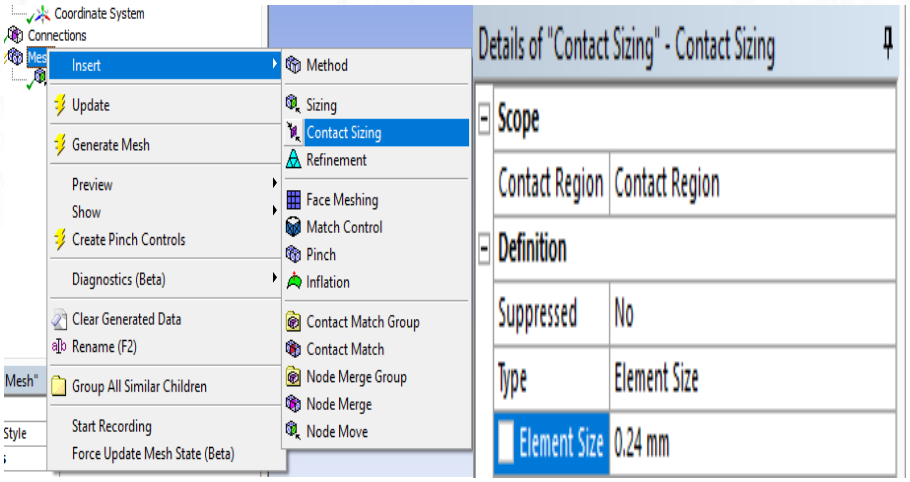

- Next, Go to **Outline** Section on left side of the window screen and right click on the body sizing and then select the **Inflation** by left click on the inflation.

- Go to the upper side of the window screen and select the **Face** option (or Ctrl + F) and then select the required face and then go to the **Detail of Inflation** section on the left side of the screen. Then, go to the **Boundary** option and left click on Apply.

Details of "Inflation" - Inflation

Scope	
Scoping Method	Geometry Selection
Geometry	2 Bodies
Definition	
Suppressed	No
Boundary Scoping Method	Named Selections
Boundary	Multiple Entities
Inflation Option	First Layer Thickness
First Layer Height	1.e-003 mm
Maximum Layers	10
Growth Rate	1.2
Inflation Algorithm	Pre

- Insert the sphere of Influence**:** Next objective was to create fine mesh to capture complete geometry in rotor bearing state region for that **sphere of influence** is used. The red coloured circular region shown is the sphere of influence.

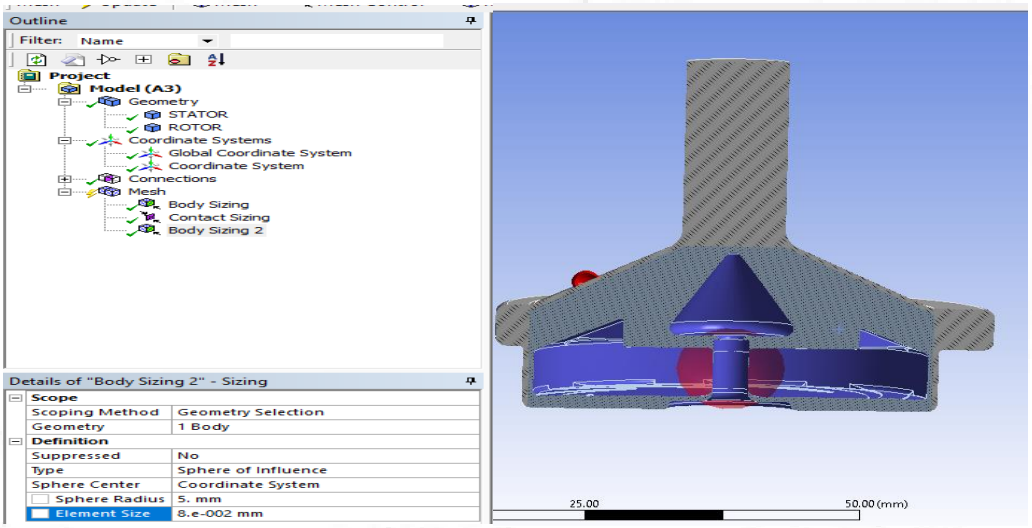

- Naming all the different parts of the extracted volume of the imported geometry to make further process more understanding and easier. Name the all faces by using face selection for giving individual face meshing and for the further analysis of surface conditions. Select the part to be named and right click and then left click on create named selection (or Ctrl+N). for example, as shown in the figure.

rotor-impeller: -

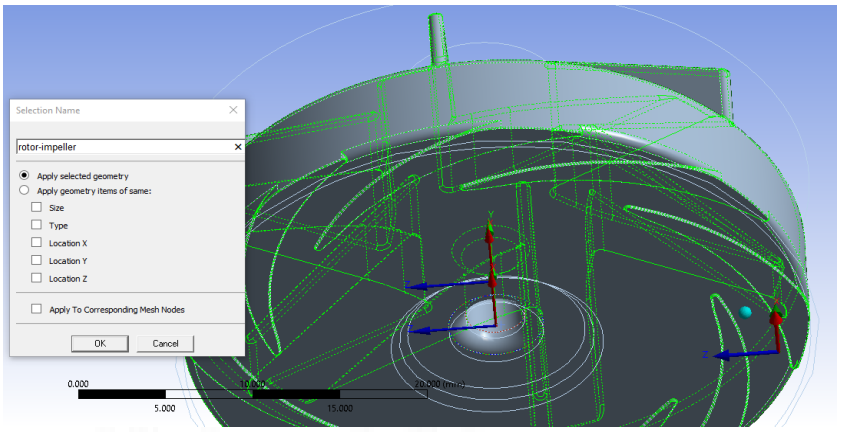

- The major named selections for the analysis of LVAD is given bellow.

Geometry name	Geometry
Rotor	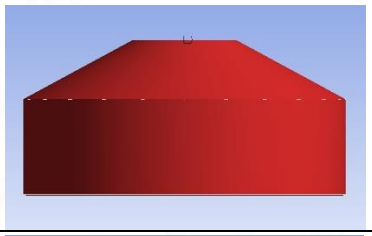
Stator	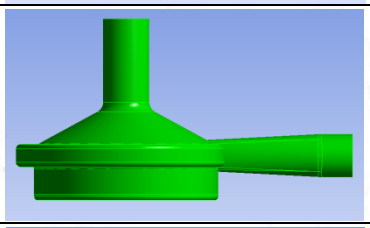
rotor-mrf-inlet-interior	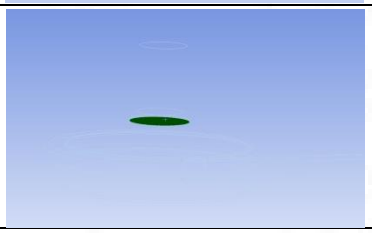
stator-outlet-pipe	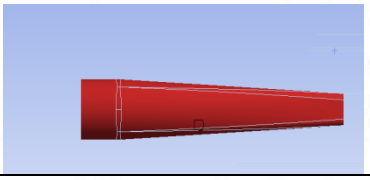
stator-casing	
rotor-bearing -stat	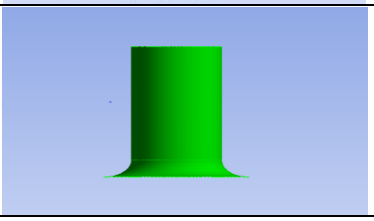

rotor-impeller-inside	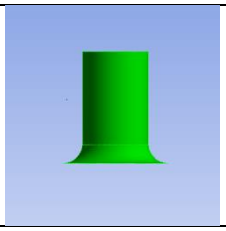
rotor-impeller	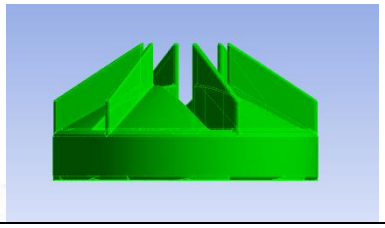
rotor-mrf-wall	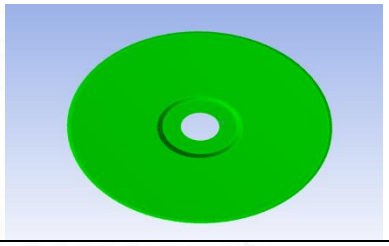
rtator-inlet-pipe	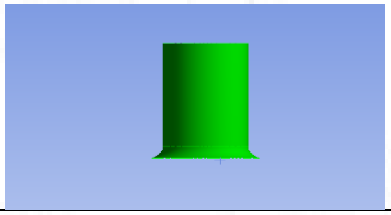
rotor-mrf-side - interior	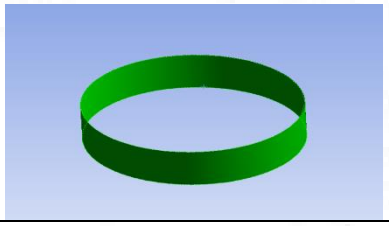
rotor-mrf-top interior	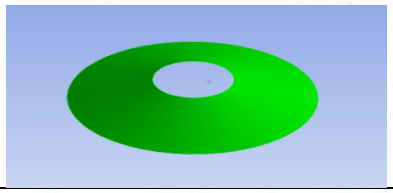
stator-inlet-mass-flow-rate	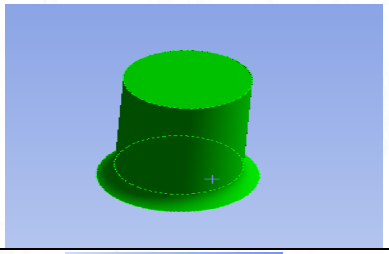
stator- outlet-pressure	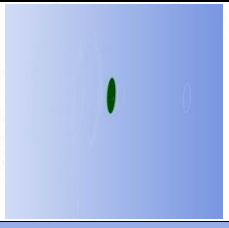
rotor-bearing-cap-stat	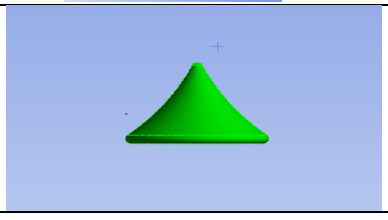

- Inserted the inflation layer and applied the conditions for inflation layer.

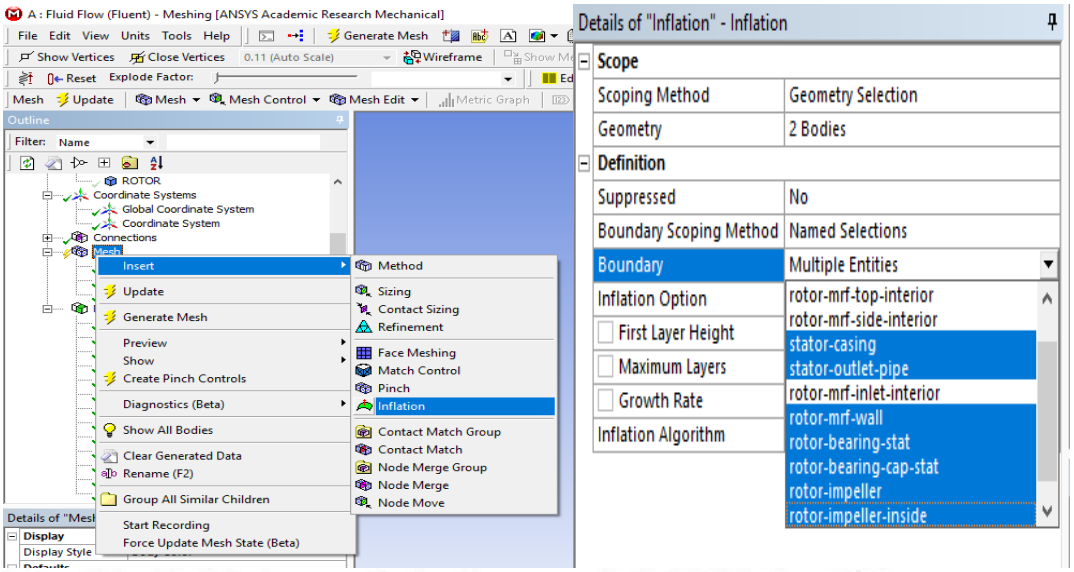

- Inserted other parameters before mesh generation as shown below.

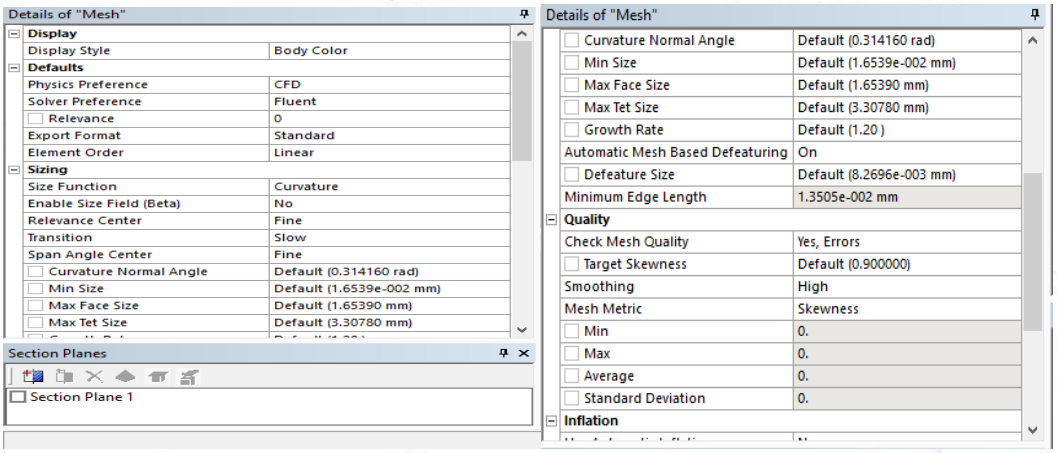

- Click on the option Generate Mesh from the top section and generated mesh is shown.

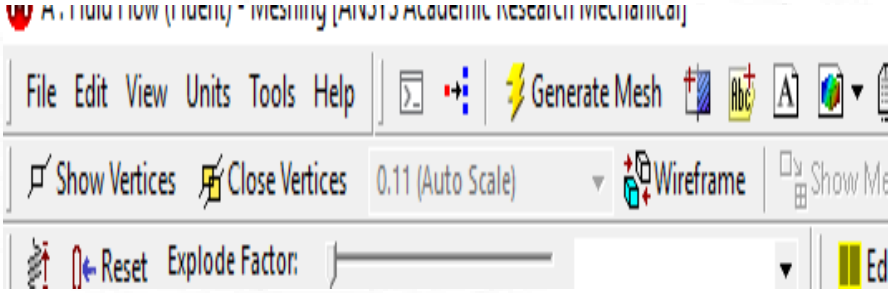

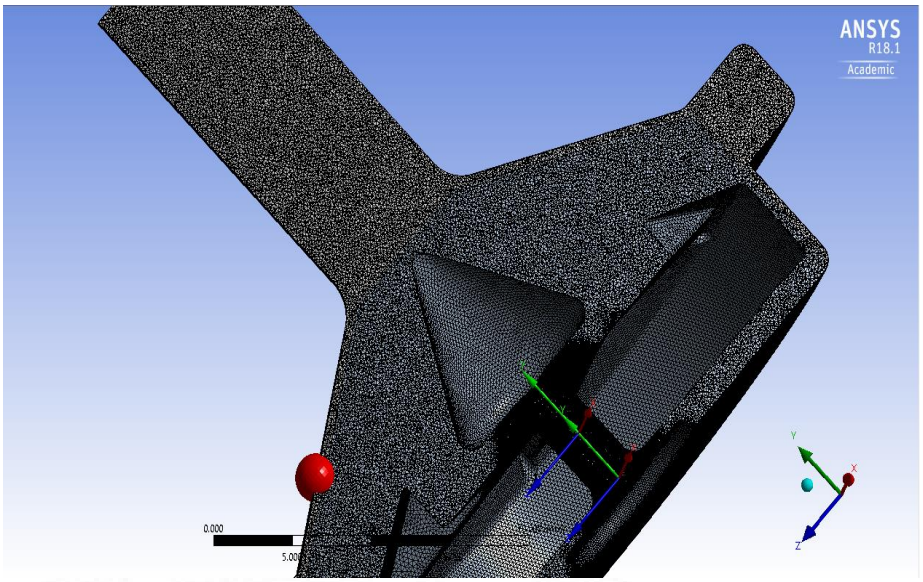

- **Step-3: Setup:**
  - Define flow models: On the left side on window under tree option left click on models and then select Viscous (Transition SST (4 eqn)). This model is used to provide more accuracy in the results.

  - Define materials: Change the property of air their to make the fluid analogous to blood and give the blood density(1056kg/m^3) and viscosity (0.0035 kg/m-s).

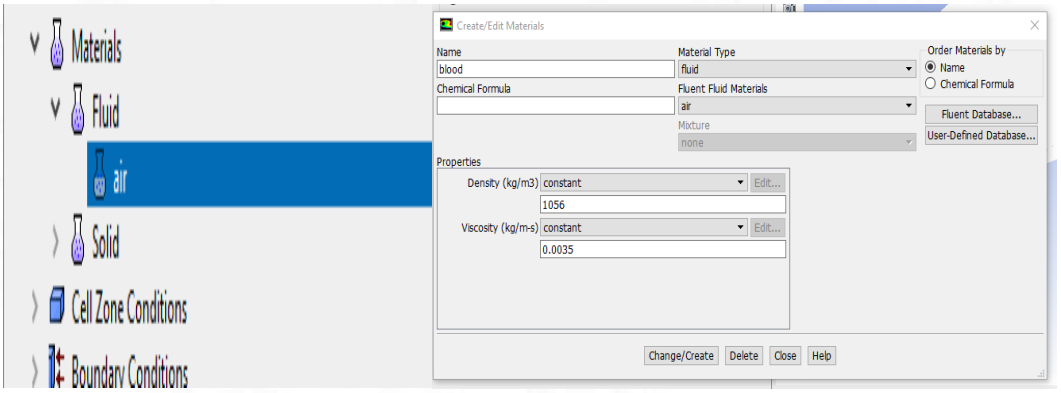

  - Define cell zone conditions: Under cell-zone condition select the rotor and select frame motion give the coordinate system that we have created for rotation under the value of X, Y, Z axis in Rotation-Axis Origin. Also provide Rotation-Axis Direction and give the value along Y-axis as -1 for clockwise direction. Assign

the speed of rotation under Rotational Velocity section as illustrated for 2500 RPM as 261.79 rad/sec.

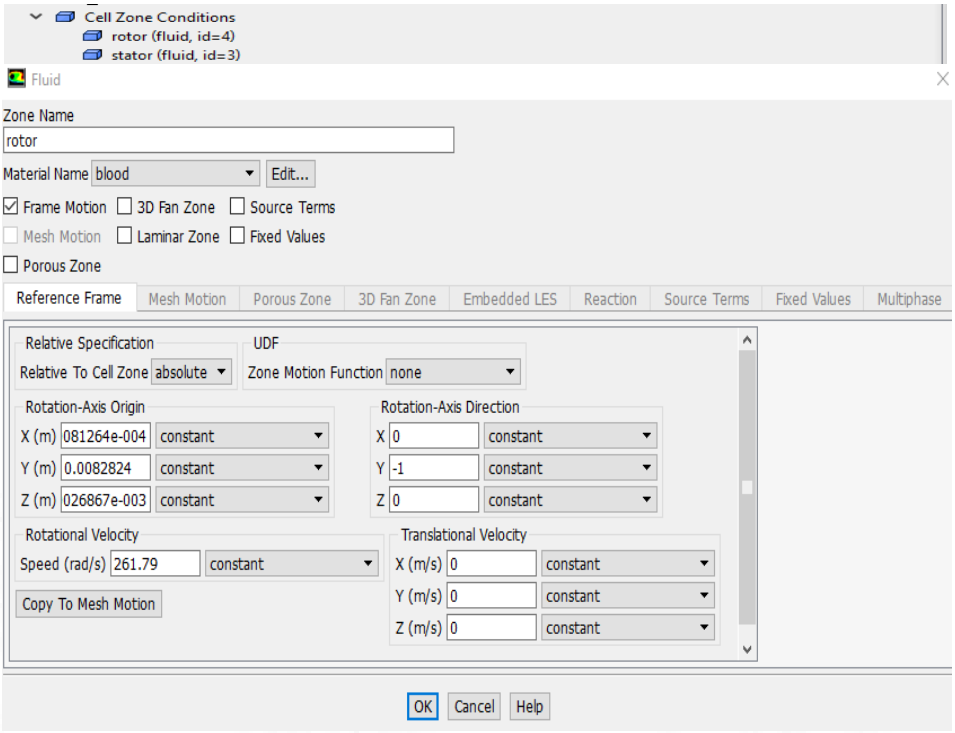

- Define Boundary Conditions:
  - Inlet Boundary Condition: Assign mass flow boundary conditions at stator-inlet-mass-flow-rate. Write mass flow rate under mass flow section as for example 5l/min as 0.08625 kg/s and change direction specification method to normal to boundary.

    for blood we know 1056 kg/m^3, then mass flow rate will be $=$

    $$\frac{\text{density of blood}}{\text{density of water}} \times \frac{\text{Liter/min}}{60} = \frac{1056}{1000} \times \frac{5}{60} = 0.08625 \text{ rad/sec}$$

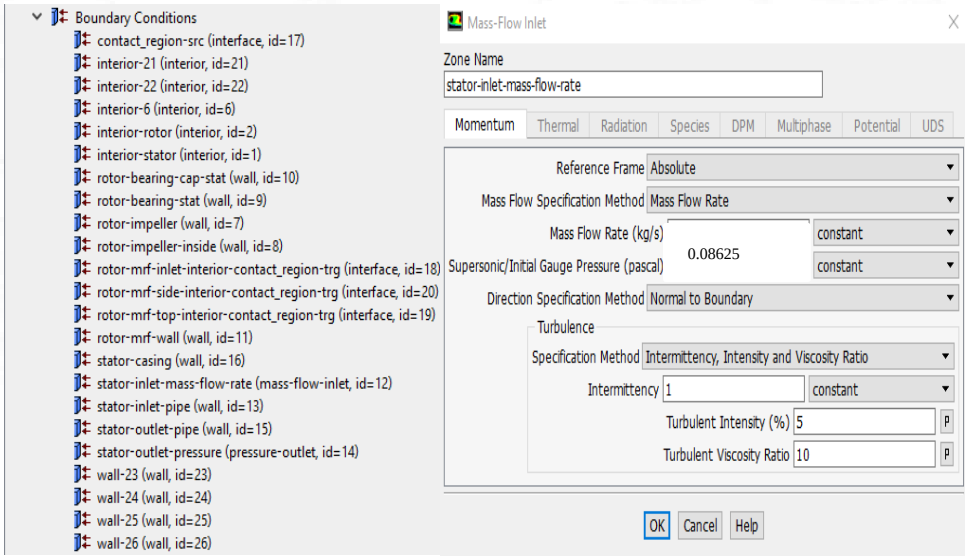

  - Outlet Boundary Condition: Assign pressure outlet at stator-outlet-pressure.

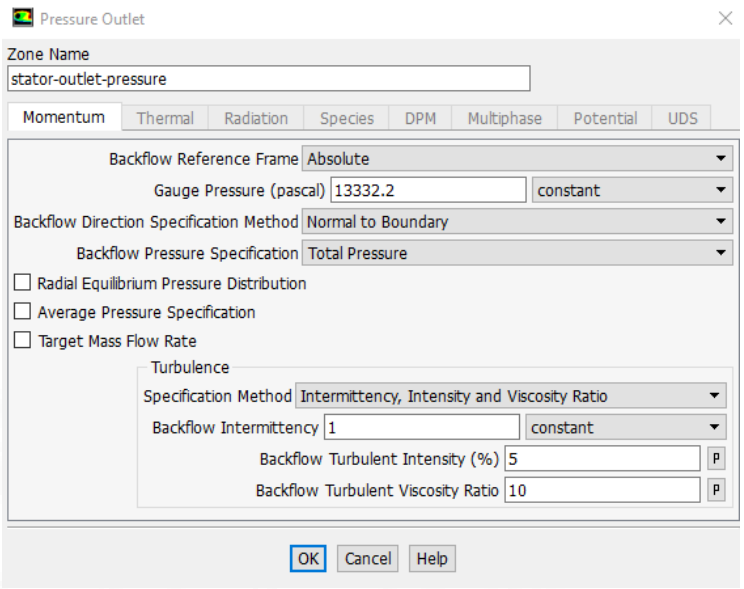

- Assign stator-inlet-pipe and stator-outlet-pipe as wall.
- Assign wall boundary conditions for all the wall surfaces.

- **Step-4: Solution:**
  - Defining solution methods: Under solution section define solution methods.

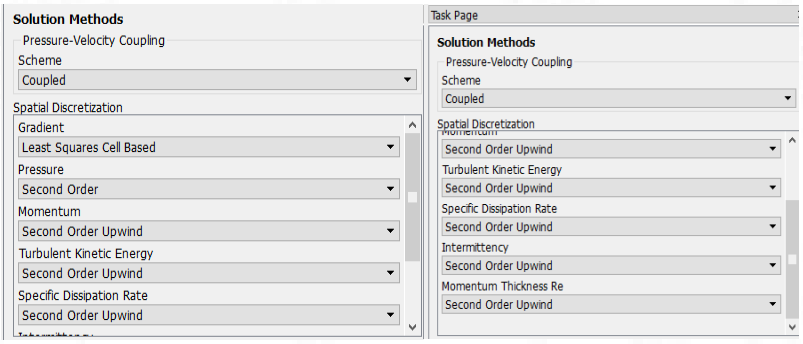

  - Defining solution Controls: Under solution control define solution control parameters.

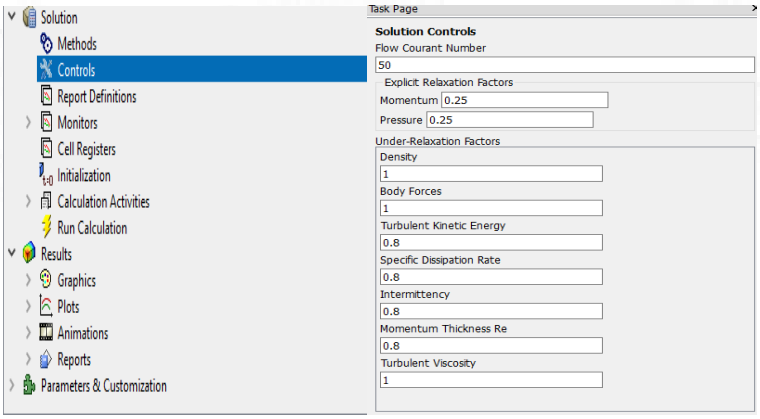

- Defining report: Create report definition as shown below:

  Report definition ⟶ New ⟶ Surface report ⟶ Area weighted average ⟶ pressure ⟶ static pressure ⟶ Inlet ⟶ OK

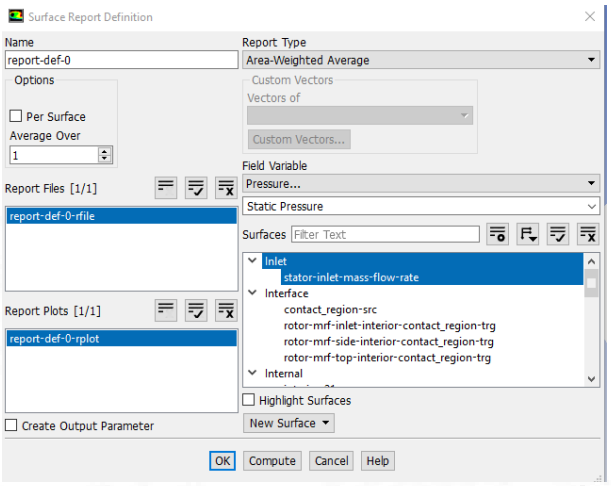

- Defining Convergence residuals:

  Residuals⟶ convergence criteria ⟶ None (It means convergence is observed by looking the graph obtained)

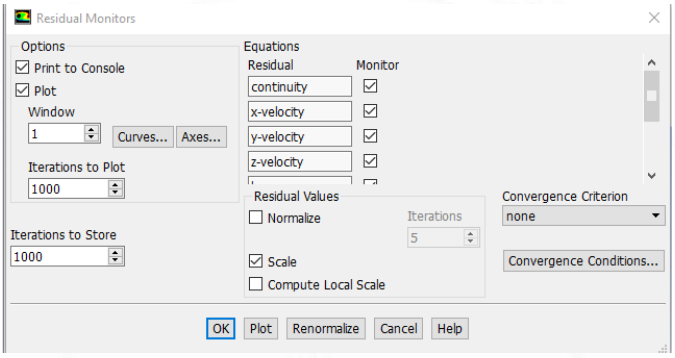

- Initialization: Selected Initialization then solution initialization then initialization methods and then hybrid initialization.

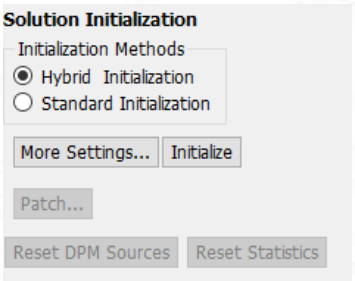

- Calculation: Selected Run Calculation option then give the minimum number of iterations required for solution to be conserved and then left click on calculate.

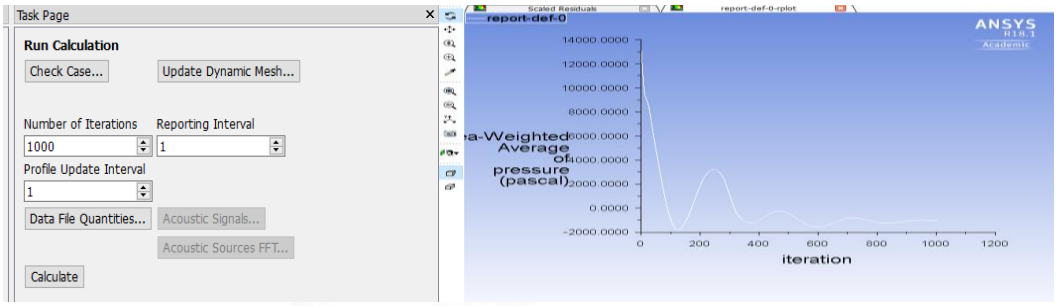

- **Step-5: Results:** Go to the function calculator under result section then selected function as torque. Then location as rotor impeller then select Axis as Global (Y) and fluid as blood then left click on calculate to get the desired value of the torque.

    - For e.g., Here RPM = 2500, Flow = 5l/min, Pressure = 100mmhg, T=9.8mN-m

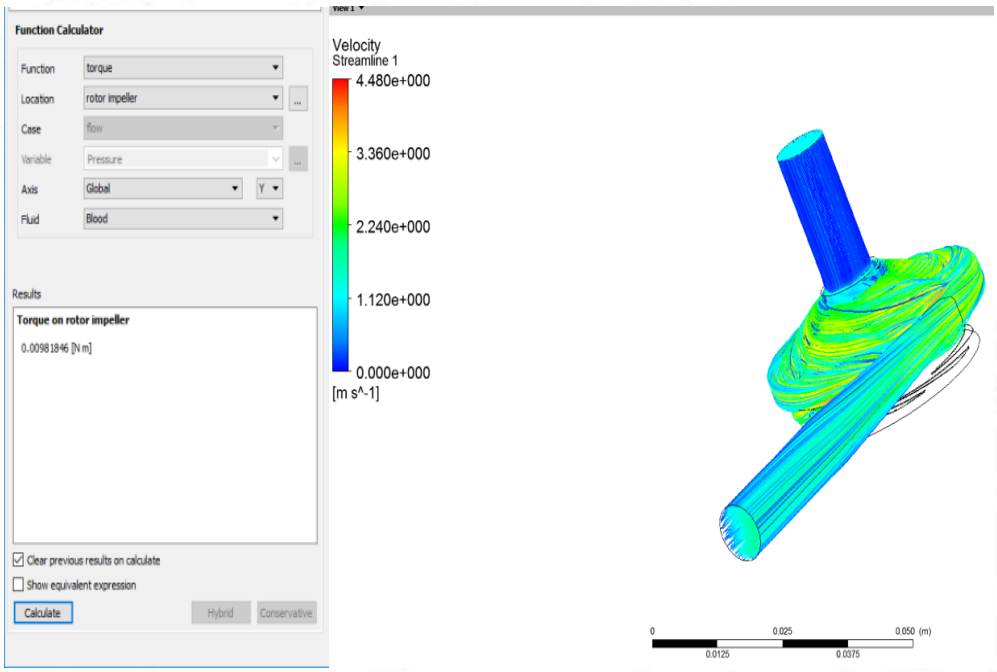

The results obtained from CFD has been shown below in the graphs according to the following results table:

Table 4.1 CFD Simulations Results

S.No.	Speed (RPM)	Flow (L/min)	Pinlet (mmHg)	Poutlet (mmHg)	ΔP (Poutlet-Pinlet)
1	3000	10	35.2	100	64.8
2	3000	9	5	100	95
3	3000	8	-15.5	100	115.5
4	3000	7	-34.1	100	134.1
5	3000	6	-49.4	100	149.4
6	3000	5	-57.8	100	157.8
7	3000	4	-64.3	100	164.3
8	3000	3	-58.7	100	158.7
9	3000	2	-62.9	100	162.9
10	3000	1	-51.5	100	151.5
11	2500	10	99.2	100	0.8
12	2500	9	78.2	100	21.8
13	2500	8	53.4	100	46.6
14	2500	7	30.4	100	69.6
15	2500	6	19.9	100	80.1
16	2500	5	-0.7	100	100.7
17	2500	4	-7.8	100	107.8
18	2500	3	-13.4	100	113.4
19	2500	2	-11.2	100	111.2
20	2500	1	-2.3	100	102.3
21	2000	10	161.06	100	-61.06
22	2000	9	130.8	100	-30.8
23	2000	8	102.1	100	-2.1
24	2000	7	84.8	100	15.2
25	2000	6	66.1	100	33.9
26	2000	5	50.4	100	49.6
27	2000	4	39.1	100	60.9
28	2000	3	32.2	100	67.8
29	2000	2	29.4	100	70.6
30	2000	1	23.1	100	76.9
31	1500	10	214	100	-114
32	1500	9	174.3	100	-74.3
33	1500	8	146.5	100	-46.5
34	1500	7	124.1	100	-24.1
35	1500	6	103.9	100	-3.9
36	1500	5	89.5	100	10.5
37	1500	4	77.3	100	22.7
38	1500	3	67.4	100	32.6
39	1500	2	62.7	100	37.3
40	1500	1	61.9	100	38.1

Graphs obtained from the above results:

- **H (Pressure Head)-Q (Flow Rate) Curve at different speed (RPM) plotted as:**

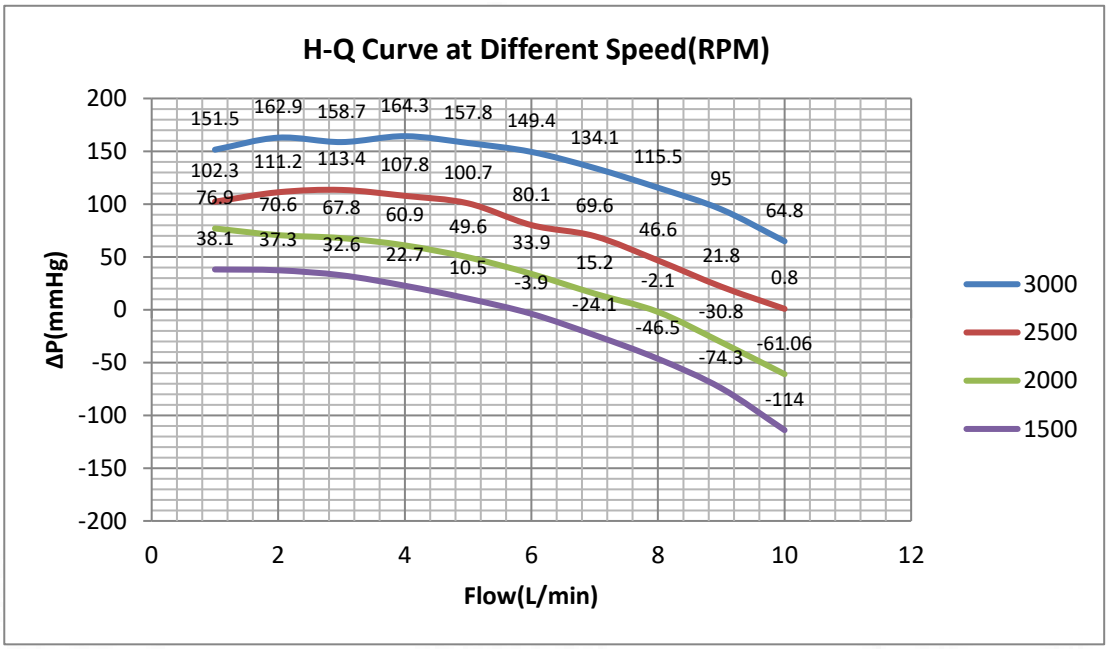

Figure 4.2 H-Q Curve at different Speed

The H-Q Curve obtained from the simulations were compared with the hydraulic performance data which was available in the lab. The comparison of the experimental and simulation data shown below in table 4.2 and % error is calculated.

Table 4.2 Percentage error in hydrodynamic performance (H-Q curve)

				Pressure (mmHg)	
S.No.	**Speed (RPM)**	**Flow (L/min)**	**Experimental**	**Simulation**	**% Error**
1	2500	5	94.7	100.7	-5.96
2	2500	4	106	107.8	-1.67
3	2500	3	113	113.4	-0.35
4	2500	2	127	111.2	14.21
5	2500	1	119	102.3	16.32

% Error has been computed as:

$$\%\text{Error} = \frac{(\text{Experimental Value} - \text{Simulation Value})}{(\text{Simulation Value})} \times 100$$

Here the maximum % error in the simulation and experimental readings was computed as 16.32. Since the error was not too much so the method considered as a good approach to take further for calculation of torque for Chitra LVAD at 2500 RPM from simulations.

The value of torque was calculated along the axis of rotation as per the co-ordinate provided for rotation and computed at 2500 RPM. The results obtained have been mentioned in the table below.

Table 4.3 Simulation Results of Torque Computed at 2500 RPM at 5 L/min

S. No.	Speed (RPM)	Flow Rate (L/min)	Torque(m-Nm)
1	2500	5	9.8

Conclusion: **The Torque obtained at 2500 RPM at 5L/min is 9.8m-Nm.**

Chapter V

Experimental Evaluation

This chapter includes the methodology adopted for the experiments that were performed, experimental set-up that was fabricated, components that were used to evaluate the experiments and the results computed from the experiments.

5.1 Methodology for Experiment

For measuring the torque, the idea of Rope Brake Method was used through which torque was computed and so was the efficiency of the BLDC motor of Chitra LVAD. The exact methodology that was used for experiments are discussed later in this chapter; first rope brake method has been discussed in brief.

Rope Brake Method:

In this method for any DC motor a rope is used to wound round the rotating structure in which one end of the rope is attached to the spring balance and the other end is carrying some load which having certain mass as shown in the figure below.

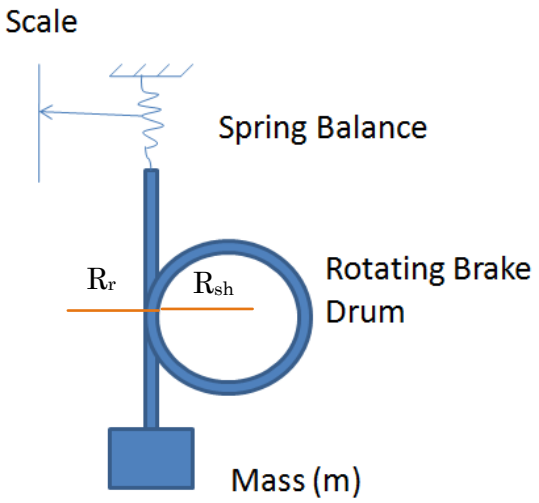

Figure 5.1 Rope Brake Method

If the rotating structure having radius R_{sh} and the rope having radius R_r then the equivalent force F_{eq} acting equals to,

$$F_{eq} = F_{gravitational} - F_{spring\ balance}$$

$$F_{eq} = mg - F_{spring\ balance}$$

Then for a rotating structure, $\tau = (F_{eq}) \times (R_{eq})$ Where $R_{eq} = R_{sh} + R_r$

Here, Output obtained is mechanical and input is electrical, so by calculating torque one can easily calculate the efficiency of the motor which is equals to the ratio of output power (mechanical) to the input power (electrical).

In Chitra LVAD same methodology was used by making a groove on the bottom side of impeller. Spring balance and mass was replaced by force sensor and a nut and bolt mechanism for the measurement of torque.

5.3 Components used for experiment

For experiment to be performed following components were used:

- Digital Force Sensor: A force sensor was used to sense the applied load on impeller from the rope so that the required force and torque was calculated.
- Acrylic sheets: For to made following assembly for the experimental setup, acrylic sheets of different thickness were used:

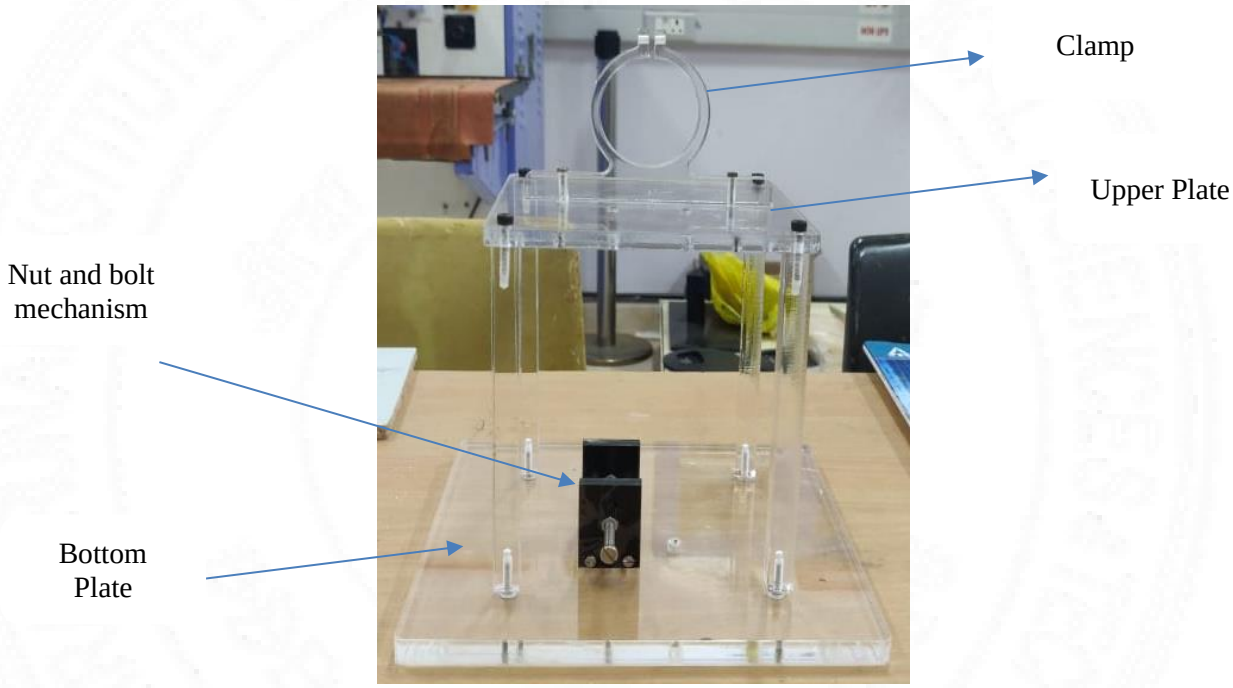

Figure 5.2 Full Assembly Prototype for Experiment

- Clamp: Clamp was used to hold the LVAD Casing which have motor and impeller attached.
- Upper and bottom plate: There two plates were used in the assembly (bottom having length L then upper plate having length L/2)
- Supporting pillars: Pillars were needed to connect and support the upper and bottom plates.
- Nut and bolt mechanism: For Fixing one side of rope, a nut and bolt mechanism was used and this mechanism was also made with the help of acrylic sheets.

- Rope: Cotton rope was used for performing the experiment.

Figure 5.3 Cotton Rope

- Nut and Bolt: For varying the load and fixing the rope nut and bolt type mechanism was used.

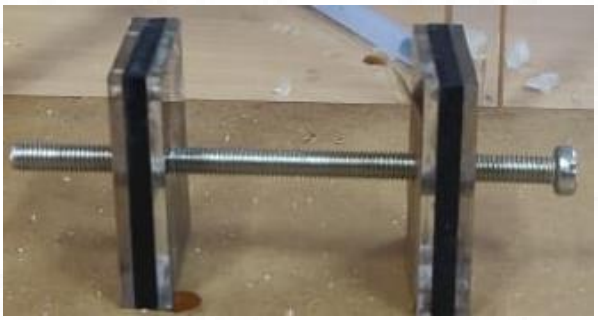

Figure 5.4 Nut and Bolt Mechanism

- Impeller with groove: A impeller which was having groove at the bottom side with the magnets attached to it was needed to perform the methodology on the experimental set-up.
- Motor Assembly: DC brushless motor with hall sensor was used to rotate the impeller. Hall sensor was used to maintain the regulation of commutator principle in the brushless DC motor through feedback pulse to the electronic speed BLDC controller which has been used as commutator for BLDC motor.
    - BLDC Motor that was used in the experiment have following properties:
        i. Connected in star connection.
        ii. It can produce 10 m-Nm of torque at 1 A.
        iii. Having NI equals to 250.

- LVAD controller: LVAD controller was used to provide the power supply to the motor and also worked as speed regulator which interfaced between power supply and LVAD motor.
- Cathode Ray Oscilloscope (CRO): Frequency was computed from CRO which helped in calculation of speed of rotation. Speed in the RPM was computed by multiplying frequency (Hz) by known factor K (K=30).

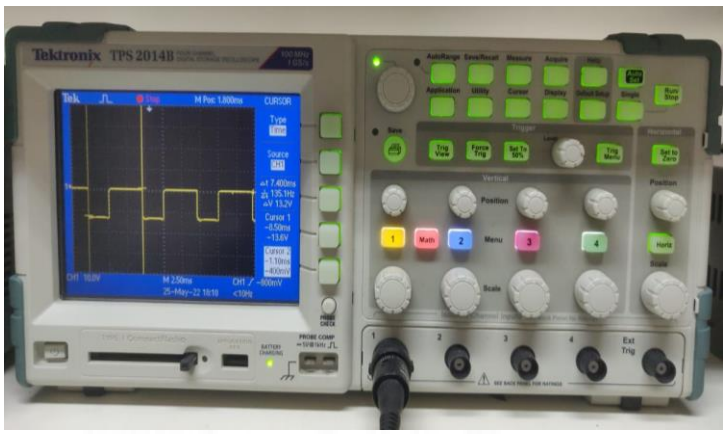

Figure 5.5 Cathode Ray Oscilloscope (CRO)

- Programmable power supply: Power supply was used to provide the power to LVAD controller to start the motor.

Figure 5.6 Programmable Power Supply

- Leads and Probes: Leads and probes was used for making connections throughout the setup either via CRO or via power supply.

All the above components were assembled together to make the required experimental setup. The techniques and software's that were used in fabrication are discussed below:

1. PTC CREO Parametric: PTC Creo software was used for making the protype device. The structural design of the prototype was first made on Creo software. The components such as Upper plate, Bottom plate, Clamp, supporting pillars, Nut and Bolt mechanism were designed on Creo software with proper dimensions required for the prototype. Then after all parts had been made, drawings were drawn for all the components for laser cutting. In the last, all parts were joined together for experimental set-up as shown below in the figure 5.7.

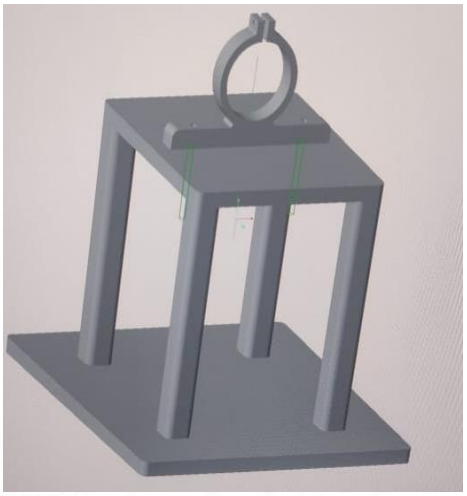

Figure 5.7 Model Designed using PTC Creo Parametric

2. Laser cutting: Laser cutting was used to cut the acrylic sheet as per the drawings drawn in PTC CREO software with proper dimensions.

5.4 Experiment Set-Up

Block Diagram:

The connections as well as the components assembled are shown in the following block diagram.

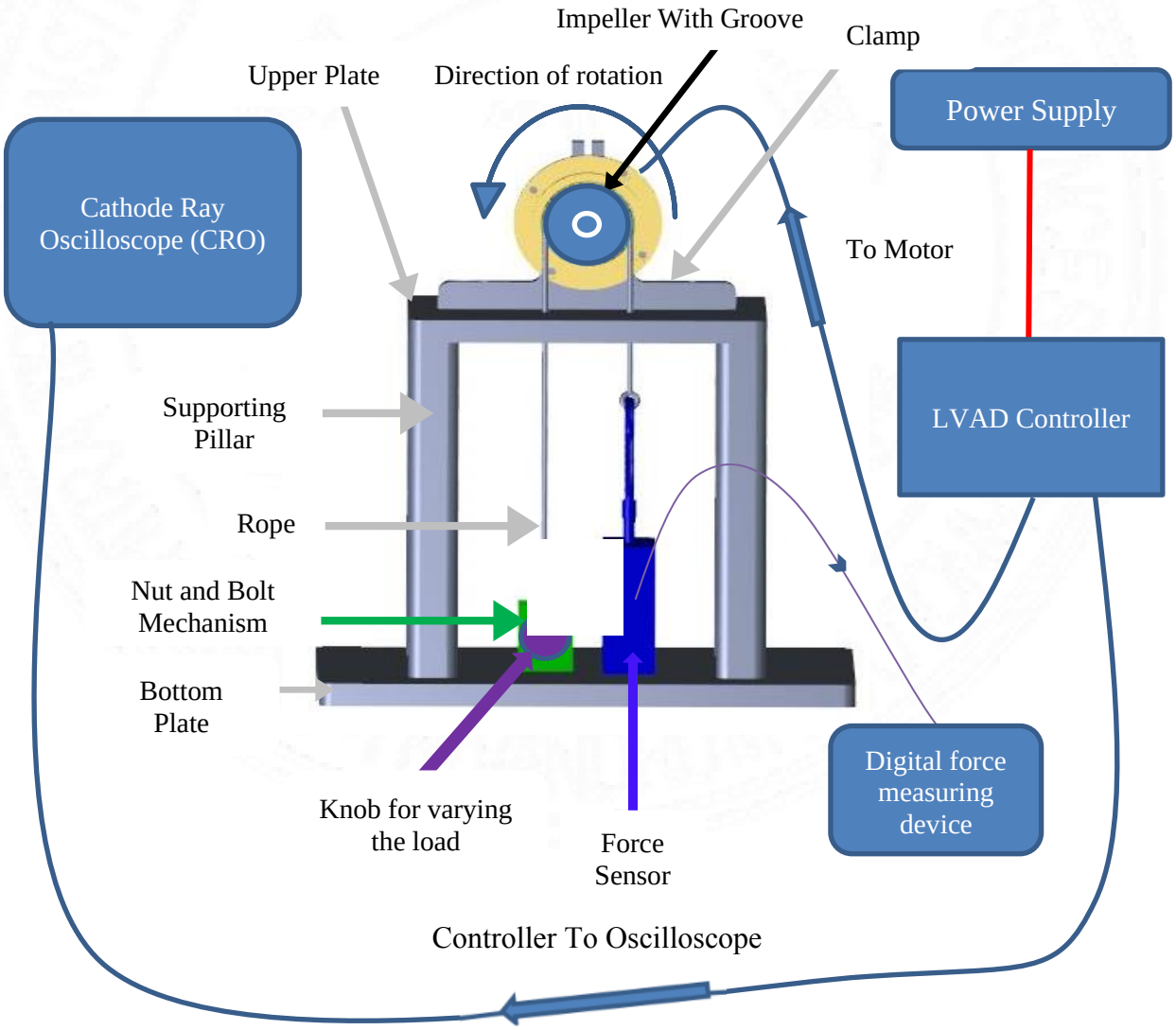

As visible in the above block diagram the whole setup has been shown which described the connection of all components for force measurement. The torque is then computed by multiplying the radius of impeller with force that was measured from the adopted method.. After torque computation electrical efficiency was calculated. The Experimental Set-up has been shown below in the figure.

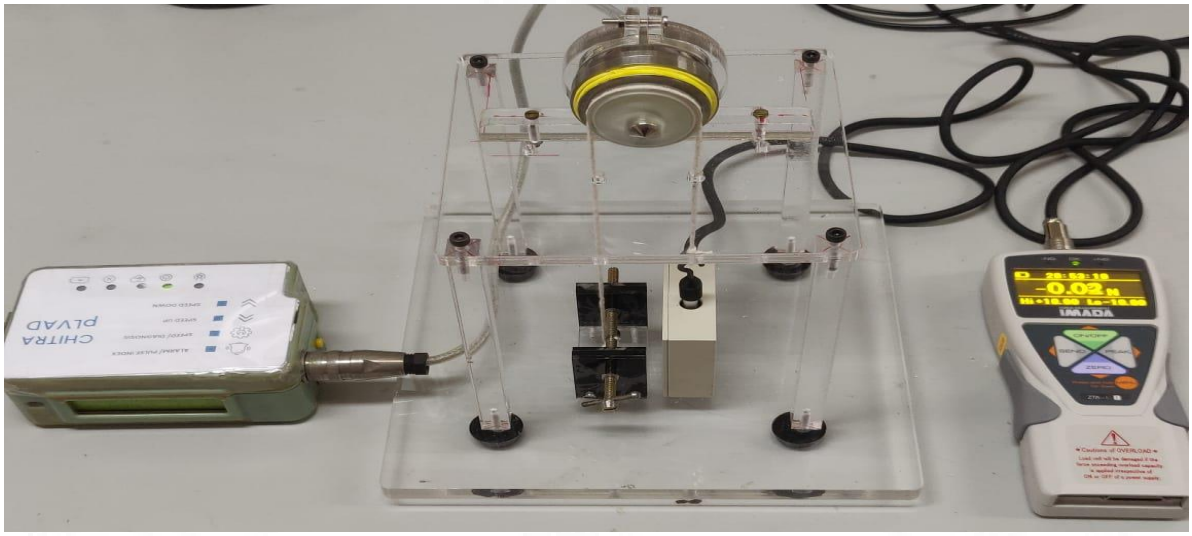

Figure 5.8 First Designed Prototype for Measurement of Torque

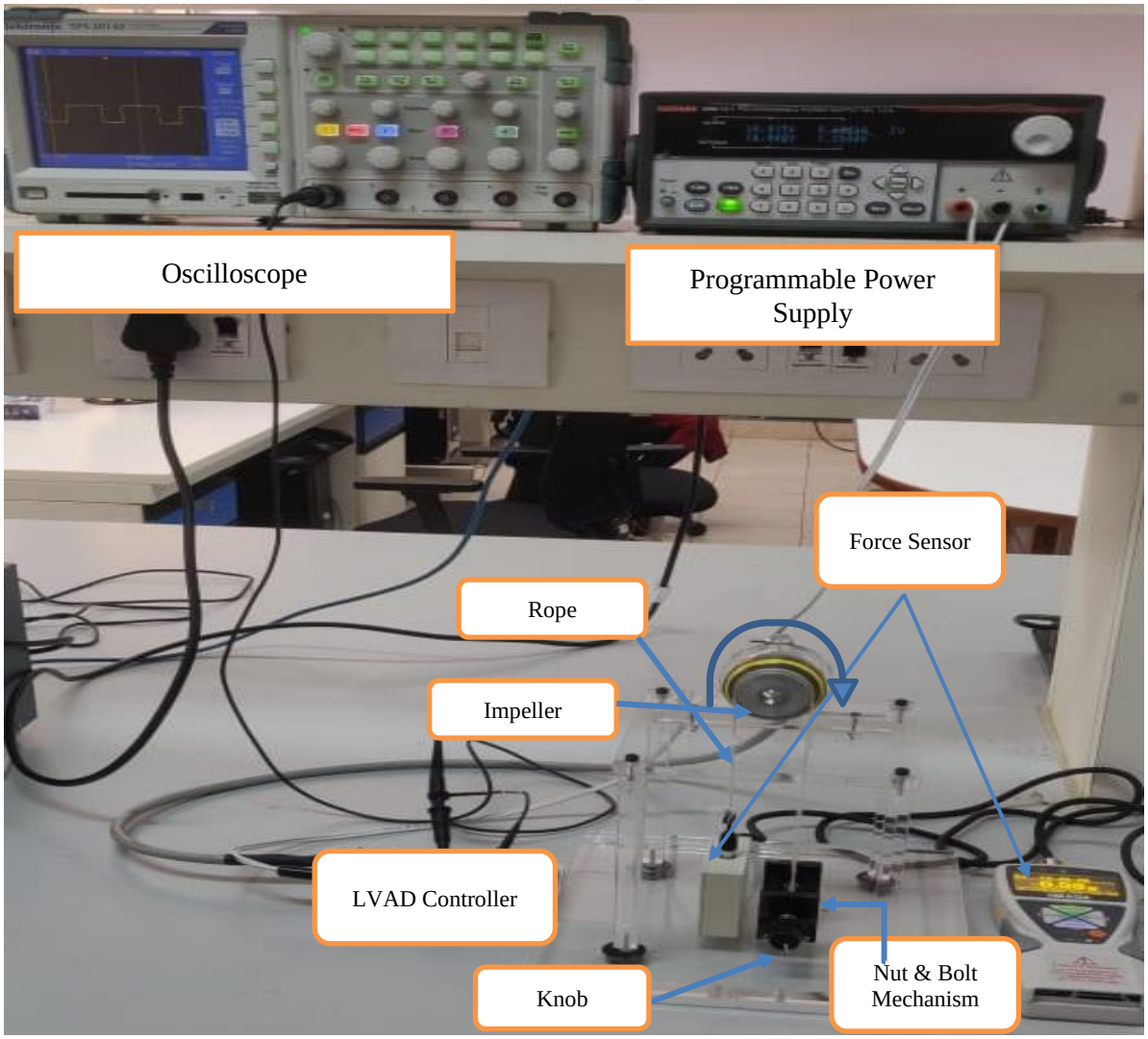

Figure 5.9 Modified Prototype (final design) with all components

Working Procedure:

The torque was calculated via force measured through digital forced sensor that was attached at one side of rope. Other side of rope was used for applying the load through nut and bolt mechanism.

The motor of the LVAD was connected to the LVAD controller which connected to the power supply from where motor provided the input power. LVAD controller was also connected to the CRO through which speed of the impeller was computed. Torque was computed with the multiplication of force (computed from force sensor) with the radius of impeller.

$$\text{Torque} = \text{Measured Force (N)} \times \text{Radius of Impeller to the point of force applied(m)}$$

And the efficiency was calculated as:

$$\text{Efficiency}(\%) = \frac{\text{Ouput Power (Mechanical)}}{\text{Input Power (Electrical)}} \times 100$$

$$\text{Where, Output Power} = \frac{2\pi NT}{60} \text{ Watts}$$

$$\text{Here, N} = \text{Revolutions Per minute}$$

$$\text{T} = \text{Measured Torque (N} - \text{m)}$$

$$\text{and Input Power} = \text{Voltage (Volts)} \times \text{Current(Amperes)} = \text{VI Watts}$$

Calibration of force sensor: Calibration of force sensor done with the help of weights that were hanged over the force sensor in the position shown below in the figure 5.22.

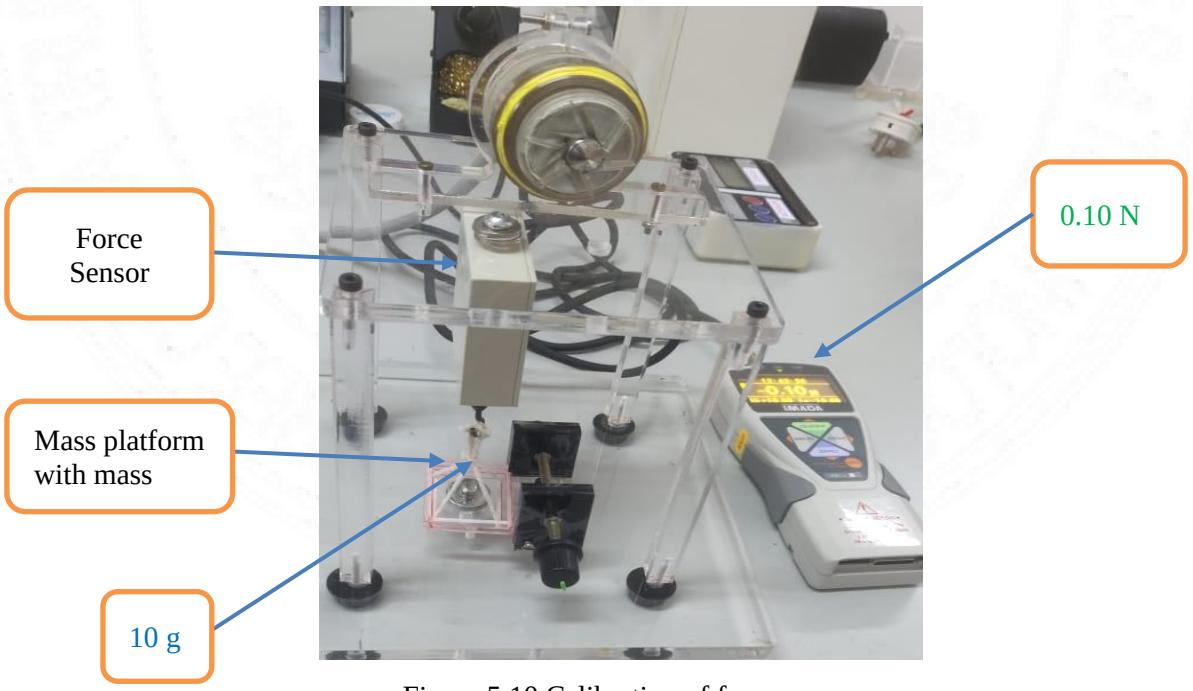

Figure 5.10 Calibration of force sensor

The results obtained from calibration of force sensor are shown below in the table 5.1:

Here the mass of platform was not considered and this was done by making zero point corresponding to mass platform with respect to force sensor.

Table 5.1 Calibration table for force sensor

S.NO.	Mass Labelled (g)	Actual Force (N)	Force Measured (N)				Error (%)
			Test-1	Test-2	Test-3	Average	
1	1	0.01	0.01	0.01	0.01	0.01	0
2	2	0.02	0.02	0.02	0.02	0.02	0
3	3	0.03	0.03	0.03	0.03	0.03	0
4	4	0.04	0.04	0.04	0.04	0.04	0
5	5	0.05	0.05	0.05	0.05	0.05	0
6	6	0.06	0.06	0.06	0.06	0.06	0
7	7	0.07	0.07	0.07	0.07	0.07	0
8	8	0.08	0.08	0.08	0.08	0.08	0
9	9	0.09	0.09	0.09	0.09	0.09	0
10	10	0.10	0.1	0.10	0.10	0.10	0
11	11	0.11	0.11	0.11	0.11	0.11	0
12	12	0.12	0.12	0.12	0.12	0.12	0
13	13	0.13	0.13	0.13	0.13	0.13	0
14	14	0.14	0.14	0.14	0.14	0.14	0
15	15	0.15	0.15	0.15	0.15	0.15	0
16	16	0.16	0.16	0.16	0.16	0.16	0
17	17	0.17	0.17	0.17	0.17	0.17	0
18	18	0.18	0.18	0.18	0.18	0.18	0
19	19	0.19	0.19	0.19	0.19	0.19	0
20	20	0.20	0.2	0.20	0.20	0.20	0

Conclusion: From above table it is concluded that the error in the actual and the measured reading was 0%. Instrument is 100% accurate.

5.5 Experimental Results:

Results Obtained from the experiment has been shown below in the table:

Table 5.2 Experimental Readings with Force Sensor

S.NO.	Speed (RPM)				Voltage (V)	Current (A)	Force (N)				Radius (mm)	Torque (mN-m)	Input Power(W)	Output Power (W)	Efficiency (%)
	Test-1	Test-2	Test-3	Average			Test-1	Test-2	Test-3	Average					
1	5070	4890	4785	4915	16	0.57	0.01	0.01	0.01	0.01	19	0.19	9.12	0.10	1.07
2	4470	4530	4470	4490	16	0.62	0.06	0.07	0.07	0.07	19	1.27	9.92	0.60	6.00
3	3870	3825	3975	3890	16	0.68	0.12	0.14	0.13	0.13	19	2.47	10.88	1.01	9.24
4	3480	3270	3630	3460	16	0.73	0.17	0.20	0.19	0.19	19	3.55	11.68	1.28	11.00
5	3000	2910	3270	3060	16	0.78	0.26	0.25	0.24	0.25	19	4.75	12.48	1.52	12.19
6	2670	2595	2970	2745	16	0.81	0.31	0.30	0.27	0.29	19	5.57	12.96	1.60	12.36
7	2445	2430	2490	2455	16	0.83	0.34	0.35	0.31	0.33	19	6.33	13.28	1.63	12.25
8	2160	2190	2370	2240	16	0.86	0.38	0.39	0.37	0.38	19	7.22	13.76	1.69	12.30
9	1830	1830	1920	1860	16	0.9	0.42	0.43	0.43	0.43	19	8.11	14.4	1.58	10.96
10	1410	1410	1500	1440	16	0.95	0.47	0.48	0.46	0.47	19	8.93	15.2	1.35	8.85
11	960	1140	1260	1120	16	0.98	0.53	0.53	0.50	0.52	19	9.88	15.68	1.16	7.39
12	780	1020	960	920	16	1.02	0.55	0.56	0.55	0.55	19	10.51	16.32	1.01	6.20
13	540	720	660	640	16	1.08	0.57	0.60	0.59	0.59	19	11.15	17.28	0.75	4.32
14	60	60	60	60	16	1.14	0.64	0.62	0.63	0.63	19	11.97	18.24	0.08	0.41

From the above table, characteristics curves were computed for the Chitra LVAD BLDC Motor as:

1. Torque Vs Current
2. Speed Vs Current
3. Speed vs Torque

- Torque Vs Current:

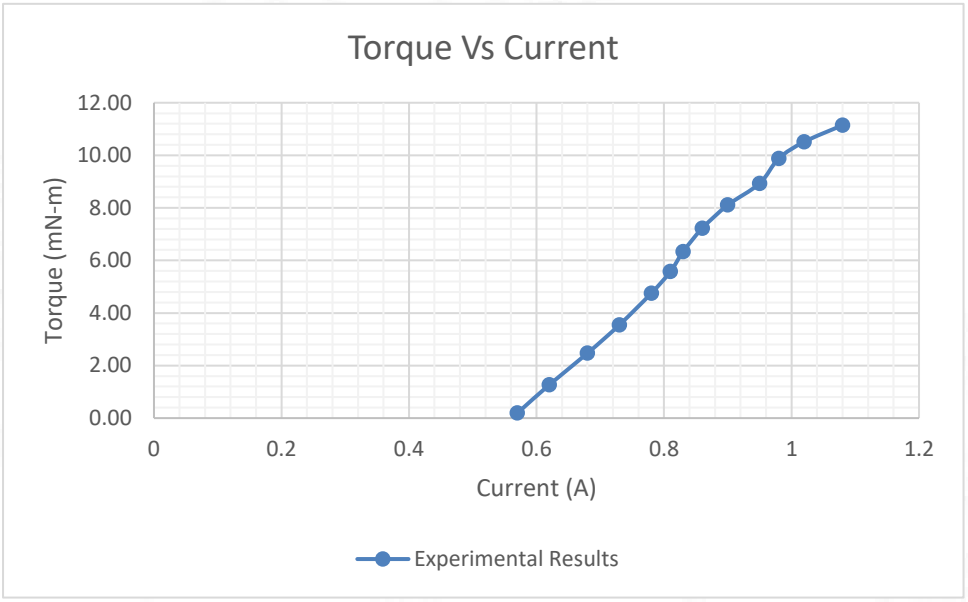

Figure 5.11 Torque Vs Current

- Speed Vs Current:

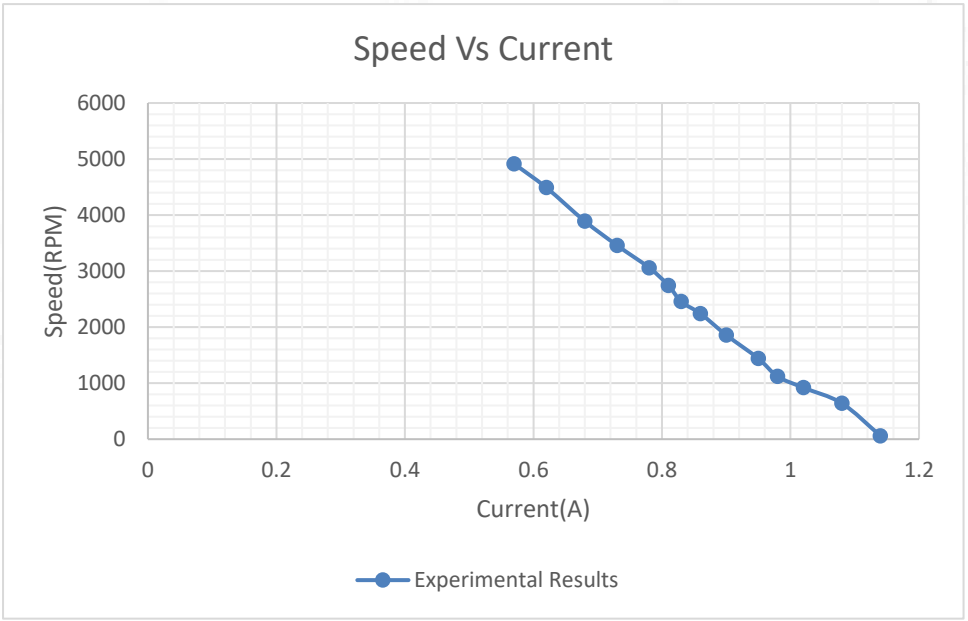

Figure 5.12 Speed Vs Current

- Speed Vs Torque:

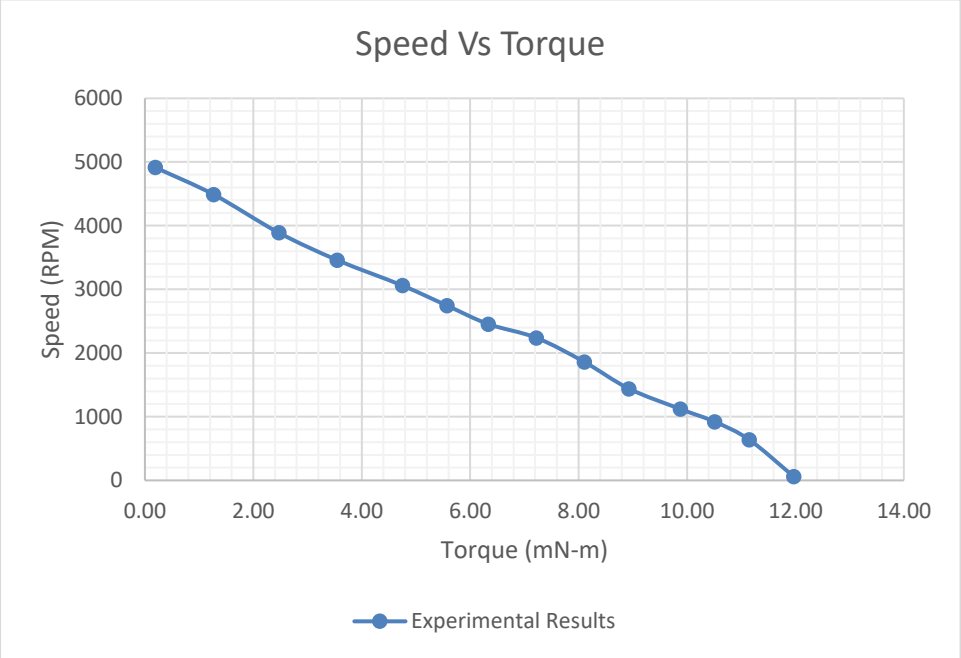

Figure 5.13 Speed Vs Torque

Same Experiment was also performed with known mass to compare the deviation of force sensor reading with the conventional measurement method. The experimental setup for this was same only one thing was replaced i.e., force sensor was replaced by 4.7 g mass platform on which known mass was placed. The technique is shown below in the figure 5.14.

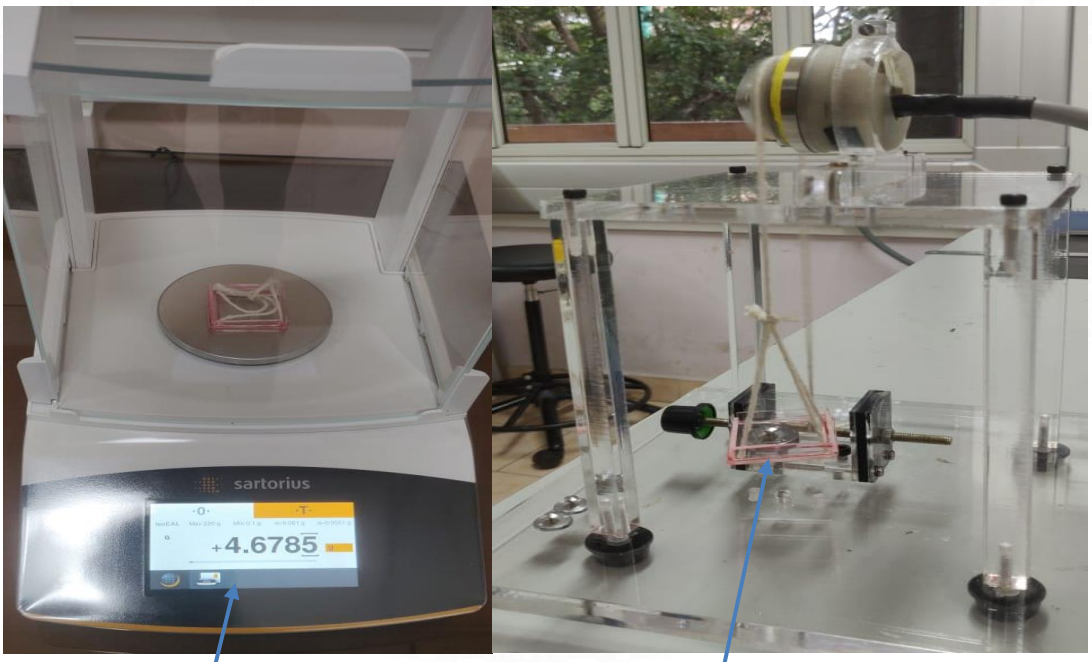

Figure 5.14 Experimental set-up with mass

Results obtained from the above experiment:

Table 5.3 Experimental Results with Weights

S.No.	Speed (RPM)				Mass	Voltage	Current(A)				Force	Radius	Torque	Input	Output	Efficiency
	Test-1	Test-2	Test-3	Average	(g)	(V)	Test-1	Test-2	Test-3	Average	(N)	(mm)	(mN-m)	Power (W)	Power(W)	(%)
1	4545	4533	4545	4541	4.7	16	0.59	0.57	0.59	0.58	0.05	19	0.89	9.33	0.42	4.55
2	4167	4251	4167	4195	9.7	16	0.64	0.62	0.63	0.63	0.10	19	1.84	10.08	0.81	8.03
3	4053	3846	3948	3949	14.7	16	0.66	0.67	0.65	0.66	0.15	19	2.79	10.56	1.15	10.93
4	3570	3060	3192	3274	19.7	16	0.7	0.73	0.7	0.71	0.20	19	3.74	11.36	1.28	11.29
5	3192	2777.7	2830.2	2933.3	24.7	16	0.73	0.78	0.75	0.75	0.25	19	4.69	12.05	1.44	11.95
6	2941.2	2419.5	2459.1	2606.6	29.7	16	0.76	0.8	0.78	0.78	0.30	19	5.64	12.48	1.54	12.34
7	2499.9	1851.9	1875.6	2075.8	34.7	16	0.82	0.87	0.86	0.85	0.35	19	6.59	13.60	1.43	10.53
8	1414.2	1505.1	1578.9	1499.4	39.7	16	0.93	0.93	0.91	0.92	0.40	19	7.54	14.77	1.18	8.01
9	980.4	1315.8	1428.6	1241.6	44.7	16	1	0.96	1	0.99	0.45	19	8.49	15.79	1.10	6.99
10	434.7	605.1	1086	708.6	48.7	16	1.11	1.09	1.09	1.10	0.49	19	9.25	17.55	0.69	3.91
11	0	0	0	0	50.7	16	1.15	1.14	1.13	1.14	0.51	19	9.63	18.24	0.00	0.00

For these results the characteristic curves of BLDC motor were plotted on graph that has been shown below:

- Torque Vs Current:

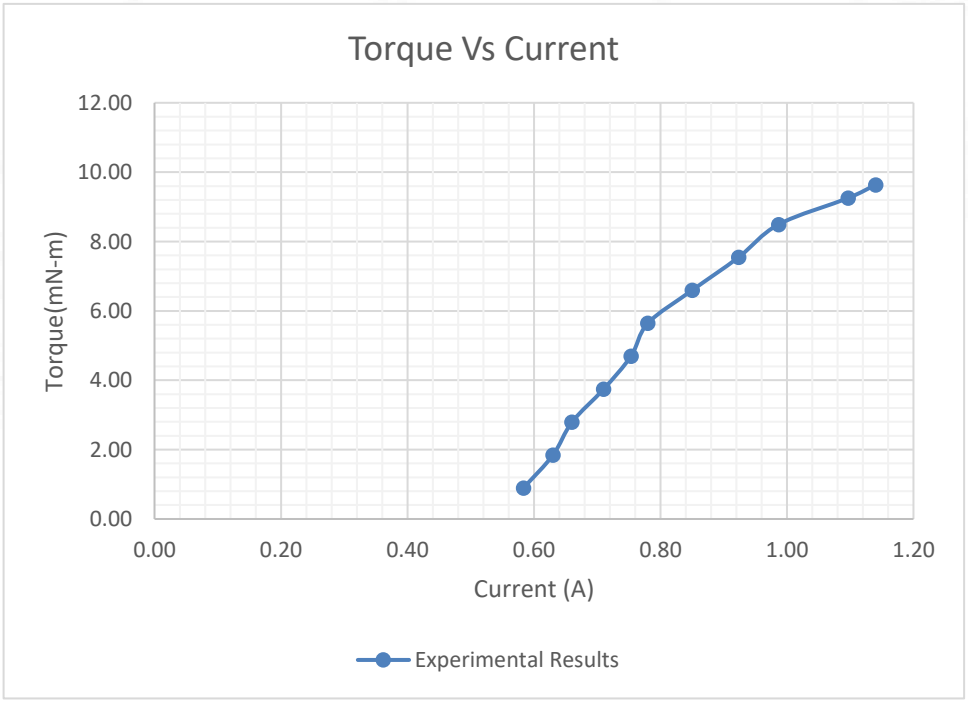

Figure 5.15 Torque Vs Current

- Speed Vs Current:

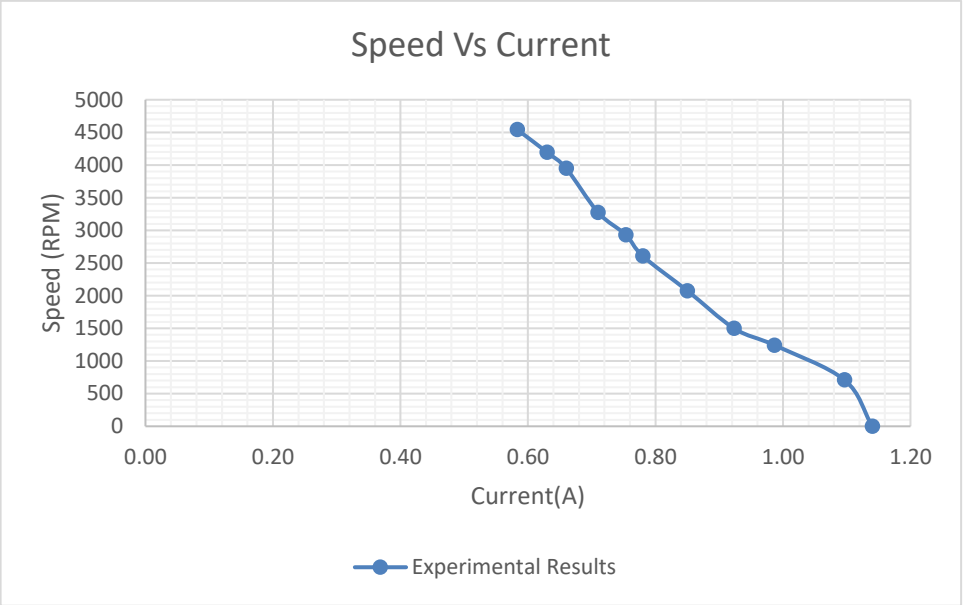

Figure 5.16 Speed Vs Current

- Speed Vs Torque:

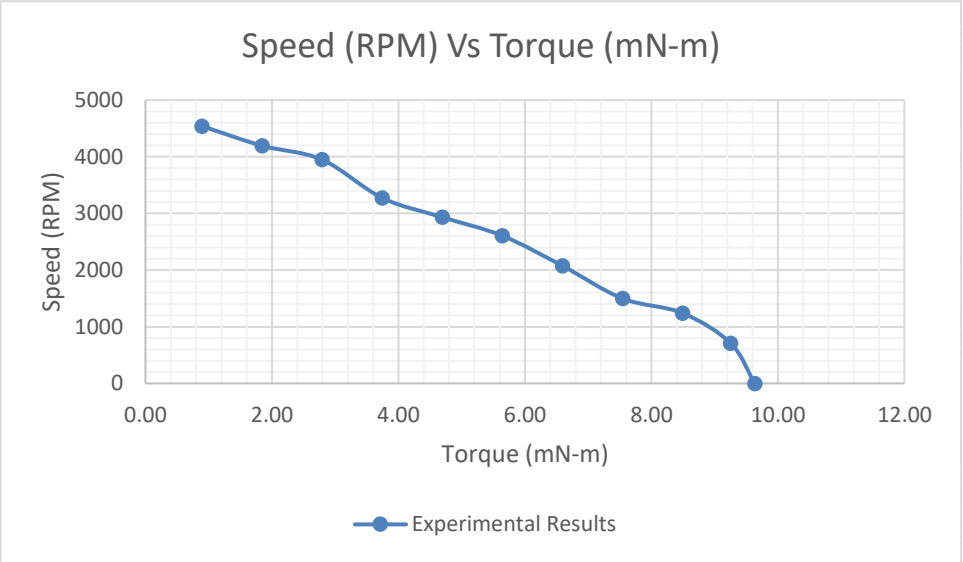

Figure 5.17 Speed Vs Torque

Limitations:

- While measuring with the mass one observation noticed that impeller rotation was decreased as we decreasing the height of the mass platform that may affect accuracy. Impeller rotation is decreased which means force on the impeller or torque was increased that happened due to certain change in the gravitational angle which led to some deflection of rope from 90 degree and readings were changed.

- Another observation was the vibrations in the rope that was also affecting the reading.

5.6 Conclusion:

The results obtained were according to the motor characteristics i.e., by applying load the armature current was increased and because of that torque was also increased. It was verified that both results are under characteristics of a DC motor.

Chapter VI

Results and Discussion

In this chapter the experimental results that were computed has been discussed thoroughly and work that can be done in the future on this project is also explained. The various conclusions obtained from different stages are also explained in this chapter.

6.1 Results

1. **Comparison of Speed Vs Torque Results obtained experimentally with Force sensor and Conventional measurement technique:**

   Torque for the Chitra LVAD was computed experimentally with the force sensor and the results verified with conventional measurement technique. The obtained results have been shown below in the graph.

   Here, the graph represented the variation of speed with torque and give a comparison curve between experiment done with the help of force sensor and conventional method. Speed which is in RPM is on the X-Axis and torque which is in mN-m is on Y-Axis.

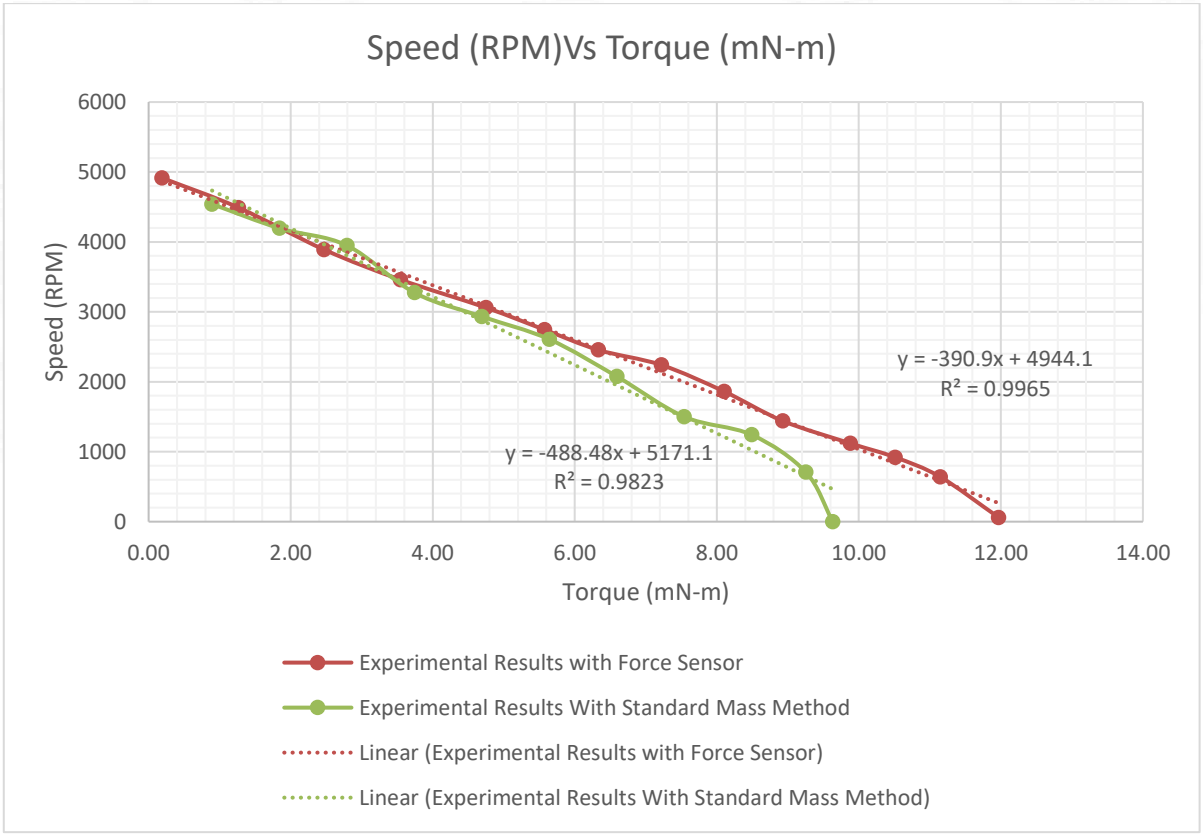

Figure 6.1 Comparison of results of known mass with force sensor

For the force sensor technique, the linear regression line equation can be written as:

$$\mathbf{Y = -390.9X + 4944.1}$$

Where, Y = Speed (RPM)
And X= Torque (mN-m)

For conventional technique, the linear regression line equation can be written as:

$$\mathbf{Y = -488.48X + 5171.1}$$

Where, Y= Speed (RPM)
And X = Torque (mN-m)

With the conventional technique, the minimum and the maximum torque computed were 0.89mN-m and 9.63mN-m. The maximum efficiency of 12.34% was obtained at speed 2606.6 RPM. On the other hand, in case of force sensor technique the minimum and maximum torque computed were 0.19mN-m and 11.97mN-m. The maximum efficiency of 12.36% was obtained at a speed 2745 RPM.

Conclusion 1: From the above results it is concluded that the force sensor can be used instead of standard conventional method for better sensitivity and accuracy.

2. **Comparison of H-Q curve calculated using Ansys simulations and Experimental data available in the lab:**

The results obtained from the simulation were compared with the experimental data available in the lab under the title hydraulic performance. The graph between experimental and simulation reading has shown below in the figure.

Here, the graph represented the H (Pressure Head) – Q (Flow Rate) curve comparison between experimental and simulation results. Pressure head (H) which is in mmHg is on the X-Axis and flow rate (Q) which is in L/min is on Y-Axis.

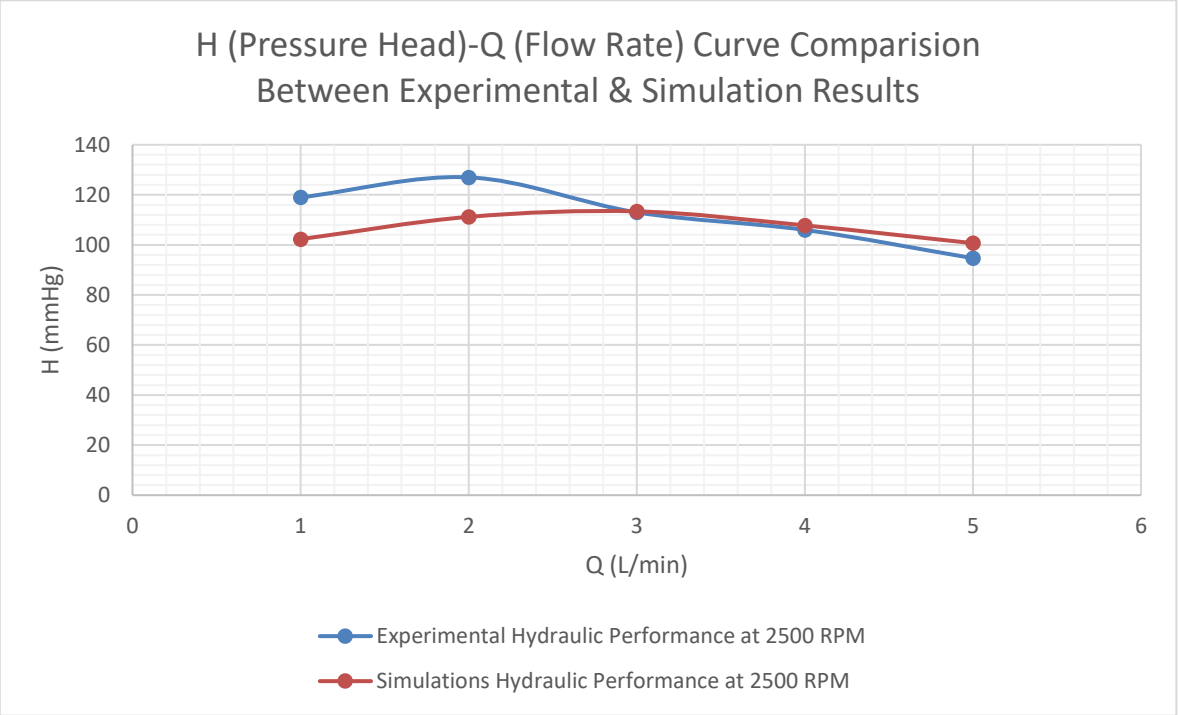

Figure 6.2 Comparison of H-Q curve Obtained from Simulation and Experimental Analysis

Conclusion 2: **It is observed from the graph that both the results were matched approximately so same methodology that was used for H-Q curve simulations can be applied to compute the torque with the help of simulations**. **The maximum error obtained between simulations and experimental readings of H-Q curve of Chitra LVAD is 16.32%.**

3. **Comparison of Torque value computed from simulation and experiment using force sensor:**

   The torque value obtained with the experiment and the simulation is shown below in the table 6.1.

Table 6.1 Comparison of the Torque value computed with the help of simulation and experiment

S. No.	Speed (RPM)	Flow Rate (L/min)	Current (A)	Torque(m-Nm)
1	2500	5		9.8
2	2500		0.83	6.33

$$\%\text{Error} = \frac{(\text{Experimental Value} - \text{Simulation Value})}{(\text{Simulation Value})} \times 100$$

$$\%\text{Error} = \frac{(6.33 - 9.8)}{(9.8)} \times 100$$

$$\%\text{Error} = 35.41$$

Conclusion 3: It is observed that the % error between the simulation and experimental analysis for Torque computation is 35.41 % at 2500 RPM.

4. **Efficiency Vs Speed Characteristics of Chitra LVAD BLDC motor:**

The graph represented the variation of electrical efficiency with different speeds. Electrical efficiency which is in % is on X-Axis and Speed which is in RPM is on Y-Axis. Here, the curve between the electrical efficiency and speed is showing that electrical efficiency first increases with the speed then became maximum and from the maximum point it decreases again. The graph is shown in figure 6.3.

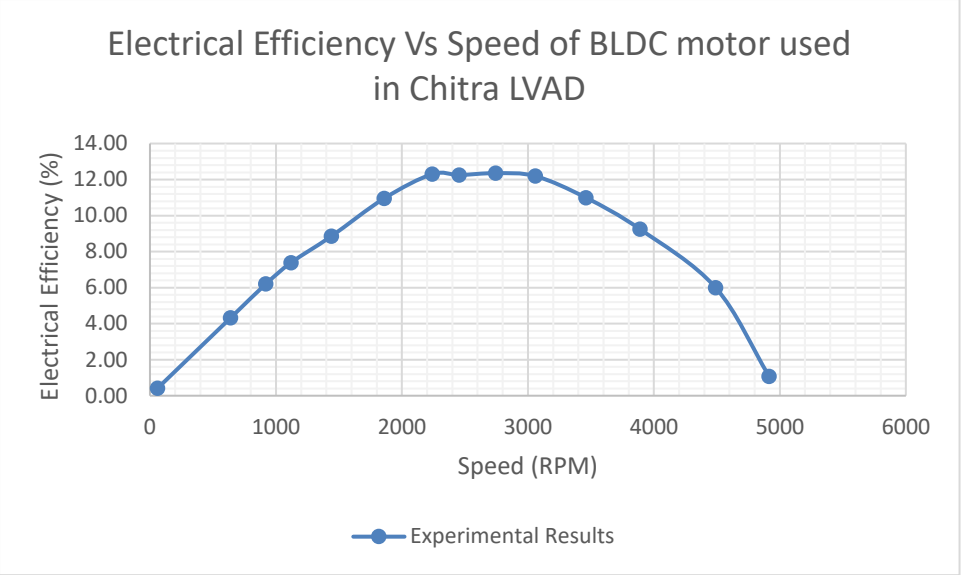

Figure 6.3 Efficiency Vs Speed characteristics of BLDC motor used in Chitra LVAD

Conclusion 4: Maximum efficiency of BLDC motor of Chitra LVAD is obtained as 12.36 % at 2745 RPM.

6.2 Future Work

The future work and the modification required for the project are listed below:

- The cotton rope used in the experiment can be replaced by non-stretchable, non-elastic conveyer belt (for e.g., we can use a part of belt which is used in flour mill industry).
- The one reason of the value coming low for weight measurement technique is vibration in the rope, height difference problem using mass platform and variable tension in the rope. By observation it has been observed that as height at load side is reduced impeller rotation or RPM is reduced which means force (gravitational) on the impeller is increased (one reason can be the deflection of angle from 90 degrees). So that part also should have to remove by some modification to get both force sensor and weight measurement readings nearly equal.
- Other electrical methods also can be used such as strain gauge method to compute the torque but need to be careful by using sensor because it may require precisely and accurately placed. It can make the torque measurement complex but method can be more accurate than the mechanical method. But it may lead to increase the cost of the experiment so the readings should be taken more carefully and precisely.
- Optical method can also be applied to measure the torque but that also needs to be more care while measuring the angle. Shaft also needed so that can increase the weight and length as well as cost of the experiment.
- Comparison of characteristics of two motor can be done with the help of same methodology.

References

1. Eisen, H., 2019. Left Ventricular Assist Devices (LVADS): History, Clinical Application and Complications. Korean Circulation Journal, 49(7), p.568.
2. Englert, Randy & Davis, Jennifer & Krim, Selim. (2016). Mechanical Circulatory Support for the Failing Heart: Continuous-Flow Left Ventricular Assist Devices. The Ochsner journal. 16. 263-9.
3. Han J, Trumble D. Cardiac Assist Devices: Early Concepts, Current Technologies, and Future Innovations. Bioengineering. 2019;6(1):18.
4. Savarese, G., & Lund, L. H. (2017). Global Public Health Burden of heart failure. Cardiac Failure Review, 03(01), 7. https://doi.org/10.15420/cfr.2016:25:2
5. Guglin M. Approach to Unresponsive Patient with LVAD. The VAD Journal. 2018;.
6. Prinzing, A., Herold, U., Berkefeld, A., Krane, M., Lange, R. and Voss, B., 2016. Left ventricular assist devices—current state and perspectives. Journal of Thoracic Disease, 8(8), pp.E660-E666.
7. Pagani, F., 2008. Continuous-Flow Rotary Left Ventricular Assist Devices with “3rd Generation” Design. Seminars in Thoracic and Cardiovascular Surgery, 20(3), pp.255-263
8. Foster, G., 2018. Third-generation ventricular assist devices. Mechanical Circulatory and Respiratory Support, pp.151-186.
9. https://cfdflowengineering.com/basics-of-cfd-modeling-for-beginners/
10. Lecture Series on Industrial Instrumentation by Prof. Alok Barua, Department of Electrical Engineering, IIT Kharagpur.
11. Fundamentals of Electric Drives by Mohammed A. El-Sharkawi
12. https://www.redbubble.com/i/canvas-print/Heart-Failure-Functional-Classification-by-Medcomic/29963648.5Y5V7
13. Zhou Q, Li P, Zhao H, Xu X, Li S, Zhao J et al. Heart Failure with Mid-range Ejection Fraction: A Distinctive Subtype or a Transitional Stage? Frontiers in Cardiovascular Medicine. 2021;8.
14. https://ctsurgerypatients.org/adult-heart-disease/left-ventricular-assist-device-lvad.

15. Miller, Jacob & Lawrance, Christopher & Silvestry, Scott. (2014). Current Options and Practices in Long-Term Ventricular Assist Devices. Current Surgery Reports. 2. 10.1007/s40137-014-0053-2.

16. Ahmed, Azzam & Wang, Xianghui & Yang, Ming. (2020). Biocompatible materials of pulsatile and rotary blood pumps: A brief review. REVIEWS ON ADVANCED MATERIALS SCIENCE. 59. 322-339. 10.1515/rams-2020-0009.

17. https://www.sctimst.ac.in/about%20sctimst/departments%20and%20divisions/BioMedical%20Technology%20Wing/Division%20of%20Extracorporeal%20Devices/

18. https://www.embibe.com/exams/torque/

19. https://en.wikipedia.org/wiki/Computational_fluid_dynamics

20. https://www.electronics-tutorials.ws/io/io_7.html

21. Moazami, Nader & Fukamachi, Kiyotaka & Kobayashi, Mariko & Smedira, Nicholas & Hoercher, Katherine & Massiello, Alex & Lee, Sangjin & Horvath, David & Starling, Randall. (2013). Axial and centrifugal continuous-flow rotary pumps: A translation from pump mechanics to clinical practice. The Journal of heart and lung transplantation: the official publication of the International Society for Heart Transplantation. 32. 1-11. 10.1016/j.healun.2012.10.001.